suppresses the HIV-1 R5 virus infection. Notably, such bimodal effects of the ERM proteins were not observed in the R5-tropic-Env-mediated cell–cell fusion (Fig. 6C). These results suggest that the ERM proteins including moesin function as positive regulators of R5-tropic-Env-mediated membrane fusion and that moesin additionally functions as a negative regulator of HIV-1 R5 virus replication at the early step(s) after the membrane fusion.

Our findings suggest that the ERM proteins regulate differently the R5- and X4-tropic HIV-1 infection. Underlying mechanisms by which the ERM proteins undergo the different regulation remain to be clarified. In this regard, CCR5 and CD4 co-localize on the plasma membrane before HIV-1 infection (Steffens and Hope, 2003, 2004), whereas CXCR4 and CD4 do not (Kozak et al., 2002). Such a difference in cell surface localization raises a possibility that regulation system for the CCR5 and CXCR4 fluidity on the plasma membrane is different. This in turn may lead to distinct regulation of infection receptor fluidity and cytoskeleton rearrangement by the ERM in CCR5 and CXCR4-mediated HIV-1 infection. However, we cannot exclude the possibility that the CCR5 over-expression in the target cells diminishes the ERM protein function for the R5-tropic HIV-1 infection (Jimenez-Baranda et al., 2007; Viard et al., 2002).

Recent study has reported that the moesin regulates stable microtubule formation and inhibits transduction of HIV-1 vectors having VSV-G protein in the rat cells (Naghavi et al., 2007). The findings suggest that moesin regulates cytoskeleton rearrangement to suppress HIV-1 replication somewhere after virus entry. Our data show that knockdown of moesin by siRNA resulted in enhancement of HIV-1 vector transduction only when the vector has the R5-tropic Env (Fig. 4C). The results suggest that in the case of R5-tropic virus infection, the moesin-mediated enhancement of infection is dominant in comparison with moesin-mediated suppression of HIV-1 replication, if any, after entry. The EZ-N protein suppressed the X4-tropic HIV-1 infection in TE671/CD4 and 293T/CD4 cells, but did not significantly in HeLa/CD4 cells (data not shown). Apparently the inconsistent results with HIV-1 vectors may imply differences of the moesin-mediated regulation system in these different cells, although further study is required for clarifying the issue.

The inhibitory effects of the ezrin dominant negative mutant and the ERM siRNAs on the HIV-1 vector transduction were not so high (about 50% reduction). As mentioned above, ERM proteins are highly homologous each other, and similarly functions, suggesting a possibility that other members of ERM family proteins complement functions of the proteins suppressed by the siRNA. Therefore, the target cells were simultaneously transfected with the siRNAs-E2, -R, and -M. However, the introduction of the three siRNAs resulted in severe cytotoxicity on the target cells as reported (Takeuchi et al., 1994), and it was difficult to analyze their effect on such cells. Transduction titers of the X4-tropic HIV-1 vectors on TE671/CD4 cells transfected with an siRNA against CXCR4, which actually reduced its expression level, was about 50% of those on the GFP siRNA-transfected cells (data not shown), like the ERM siRNAs. This result suggests that the ERM proteins function in X4-tropic HIV-1 entry as importantly as CXCR4 does.

In conclusion, we found that ezrin, radixin, and moesin proteins functions as pleiotropic regulators of HIV-1 infection in human cells. Our findings provide a basis to study HIV-1 entry in relation to the regulation of membrane protein fluidity and cytoskeleton rearrangement by the ERM proteins.

## Materials and methods

### Env protein expression plasmids

An X4-tropic HIV-1 NDK Env expression plasmid was kindly provided by Dr. U. Hazan (Dumonceaux et al., 1998). HIV-1 HXB2 (X4 tropic), JRFL (R5 tropic), NH1 (X4R5-tropic), and NH2 (R5 tropic) Env expression plasmids were kindly provided by Dr. Y. Yokomaku (Kusagawa et al., 2002; Yokomaku et al., 2004). These HIV-1 Env expression plasmids encodes HIV-1 tat and rev genes as well as the env sequence. A VSV-G expression plasmid (pHEF-VSV-G) was obtained from Dr. L. Chang through the AIDS Research and Reference Reagent Program, Division of AIDS, NIAID, NIH, USA (Iwakuma et al., 1999).

### Construction of C-terminally HA-tagged radixin expression plasmid

Total RNA samples were isolated from TE671 cells, and radixin cDNA was amplified by PCR using following primers; Rad-S (5 -GAGAAAGAAAATGCCGAAACC-3 ) and Rad-AS (5 -ATATATGCAAAATAACAGCTCTCA-3 ). The radixin PCR products were ligated into pTarget vector plasmid (Promega) by TA cloning. The predicted amino acid sequence of the radixin cDNA was completely identical to that of already reported human radixin. The radixin sequence was amplified by PCR using the Rad-S and Rad-HA (5 -TCATGCGTAATCCG-GAACATCGTACGGGTATCCCATTGCTTCAAACTCATC-3 ) for C-terminal HA tagging. The antisense Rad-HA primer contains the HA tag sequence. The PCR product was ligated into pTarget vector and its nucleotide sequence was confirmed.

### HIV-1 vector

A DNA construct (R8.91) that encodes HIV-1 proteins required for HIV-1 vector preparation except for Env protein was kindly provided by Dr. D. Trono (Naldini et al., 1996). A LacZ-containing HIV-1 vector genome expression plasmid (pTY-EFnLacZ) was obtained from Dr. L. Chang through the AIDS Research and Reference Reagent Program, Division of AIDS, NIAID, NIH, USA (Chang et al., 1999).

### Cells

Human TE671, 293T, HeLa cell lines were cultured at 37 C under 5% $CO_2$ in Dulbecco's modified Eagle's medium (Wako) supplemented with 8% fetal bovine serum (Biosource). CD4-expressing TE671 and HeLa cells (TE671/CD4 and HeLa/CD4) were constructed by transfection with a CD4-expression plasmid containing the neomycin resistant gene. CD4-expressing 293T cells (293T/CD4) were constructed by transfection with a CD4-expression plasmid containing the hygromycin resistant gene. TE671 cells expressing CD4 and CCR5 (TE671/CD4/R5) were

constructed as follows. The TE671/CD4 cells were inoculated with a CCR5 and puromycin-resistant gene-encoding murine leukemia virus (MLV) vector constructed as reported (Kubo et al., 2003), and were selected with puromycin. Puromycin-resistant cell pool was used in this study. TE671 and 293T cells expressing CD4 and a C-terminally VSV-G-tagged dominant negative mutant of ezrin (EZ-N) was constructed by inoculation of the TE671/CD4 and 293T/CD4 cells with an EZ-N-encoding MLV vector constructed as reported (Kubo et al., 2003), and designated as TE671/CD4/EZ-N and 293T/CD4/EZ-N. The VSV-G-tagged EZ-N plasmid was kindly provided from Dr. M. Arpin.

### Transduction assay

To obtain HIV-1 vector particles, 293T cells ($5\times10^5$) were plated onto a 10-cm dish and cultured for 2 days. The 293T cells were transfected with the R8.91, pTY-EFnLacZ, and one of HIV-1 Env expression plasmids. The transfected 293T cells were washed to remove the transfection complex 24 h after transfection, and continued to be cultured in fresh medium for additional 24 h. Culture supernatants of the transfected cells were diluted to make their titer about 60 blue-cell-forming units per a microscopic field in ezrin dominant negative mutant-free or siRNA-free cells, and were inoculated into target cells. Target cells ($2\times10^5$) were plated onto a 6-cm dish and were inoculated 24 h after the plating. The inoculated cells were stained with 5-bromo-4-chloro-3-indolyl- -D-galactopyranoside (X-Gal) (Wako) 2 days after inoculation. Numbers of blue cells were counted to estimate transduction titers.

### Western immunoblotting

Cell lysates were subjected to sodium dodecyl sulfate polyacrylamide gel electrophoresis (BioRad), and were transferred onto a PVDF membrane (Millipore). The membrane was treated with an anti-VSV-G (Sigma), -ezrin, -radixin, -moesin, or -actin antibody (Santa Cruz), and then with a horseradish peroxidase-conjugated protein G (BioRad). Protein G-bound polypeptides were visualized by ECL Western blotting detection reagents (Amersham Pharmacia Biotech).

### FACS

To analyze cell surface expression of CXCR4 and CCR5, suspended cells were treated with a rat anti-CXCR4 or -CCR5 antibody (Tanaka et al., 2001). The cells were washed with PBS 3 times, and then treated with an FITC-conjugated anti-rat IgG antibody (Sigma). The cells were applied to a flow cytometer (Coulter). To analyze CD4 cell surface expression, cells were treated with an FITC-conjugated anti-CD4 antibody (Sigma).

### Transfection of siRNA

Sequences of sense strands of two siRNAs against ezrin were GAAUCCUUAGCGAUGAGAUCU (siRNA-E1) and CCUGAUUCUCGCGAUUAUUCU (siRNA-E2). Sequences of sense strands of siRNAs against radixin and moesin were CGACAAGUUAACACCUAAAU (siRNA-R) and CUCCCAGACGGAUCUGUUGC (siRNA-M). An siRNA against green fluorescence protein (GFP) was used as control, and sequence of the sense strand was CUGGAGUUGUCCCAAUUCUUG. These siRNAs were synthesized by RNAi Co. LTD. Cells were transfected with one of these siRNAs (200 pmol) by the TransIT TKO reagent (10 l) (Mirus). To knockdown expression of all three ERM family proteins simultaneously, cells were co-transfected with three siRNAs (total 600 pmol) by the transfection reagent (30 l).

### Semi-quantitative RT-PCR

Total RNA was isolated from siRNA-transfected cells. First strand cDNA was synthesized from the total RNA with ramdom hexamer by a reverse transcriptase (TAKARA). Semi-quantitative PCR was performed using the first strand cDNA as template to detect ezrin, radixin, moesin, and GAPDH mRNAs. Nucleotide sequences of the PCR primers for ezrin mRNA were GCACAAACTTACCAG and TGGTCCTGGCCTGGCTGTTA, for radixin mRNA were GGCAACACAAAGCTTTTGCAG and ATATATGCAAAATAACAGCTCTCA, for moesin mRNA were TGAGGCTGTGGAGTGGCAGCA and CTAGAGGCTGGGTGCCCATTA, and for GAPDH mRNA were AGGTCGGAGTCAACGGATTTGGT and GTGGGCCATGAGGTCCACCAC. These primers were synthesized by Genenet Co. Ltd.

### Cell-fusion assay

Receptor protein-expressing cells ($2\times10^5$) were plasted onto a 6-cm dish and cultured for 2 days. The cells were co-transfected with the siRNA and a -galactosidase expression plasmid, in which the -galactosidase gene is under the control of an HIV-1 long terminal repeat (LTR-LacZ), by the TransIT TKO transfection reagent (Mirus). 293T cells ($2\times10^5$) were plated onto a 6-cm dish and cultured for 2 days. The cells were transfected with a Tat expression plasmid as control or the HIV-1 Env expression plasmid by the Lipofectamine transfection reagent (Invitrogen). The Env expression plmasids additionally encodes the tat gene. The transfected recipient cells ($5\times10^5$) were added onto the HIV-1 Env-expressing 293T cells 24 h after transfection. If these cells fuse, the Tat protein activates the -galactosidase expression. -Galactosidase activity of cell lysates was measured 24 h after mixed culture by the high sensitive -galactosidase activity kit (Stratagene).

### Statistical analysis

Differences between two groups of data were determined by the Student's t-test. Statistical significance was set at $P<0.05$ for all tests.

## Acknowledgments

We thank Dr. U. Hazan for the NDK Env expression plasmid, Dr. Y. Yokomaku for the HXB2, JRFL, NH1, and NH2 Env expression plasmids, Dr. D. Trono for the R8.91 plasmid, Dr. L. Chang for the VSV-G expression plasmid and pTY-EFnLacZ,

and Dr. M. Arpin for the expression plasmids of the wild type and dominant negative forms of ezrin. The VSV-G, TAT, and LacZ-containing HIV-1 vector genome expression plasmids were onbatined through AIDS Research and Reference Reagent Program, NIAID, NIH, USA. This study was supported by a Health Science Research Grant from the Ministry of Health, Labour, and Welfare of Japan and by the 21st century Centers of Excellence (COE) program.

## References

Algrain, M., Turunen, O., Vaheri, A., Louvard, D., Arpin, M., 1993. Ezrin contains cytoskeleton and membrane binding domains accounting for its proposed role as a membrane-cytoskeletal linker. J. Cell Biol. 120 (1), 129–139.

Chang, L.J., Urlacher, V., Iwakuma, T., Cui, Y., Zucali, J., 1999. Efficacy and safety analyses of a recombinant human immunodeficiency virus type 1 derived vector system. Gene Ther. 6 (5), 715–728.

Das, V., Nal, B., Roumier, A., Meas-Yedid, V., Zimmer, C., Olivo-Marin, J.C., Roux, P., Ferrier, P., Dautry-Varsat, A., Alcover, A., 2002. Membrane-cytoskeleton interactions during the formation of the immunological synapse and subsequent T-cell activation. Immunol. Rev. 189, 123–135.

Doi, Y., Itoh, M., Yonemura, S., Ishihara, S., Takano, H., Noda, T., Tsukita, S., 1999. Normal development of mice and unimpaired cell adhesion/cell motility/actin-based cytoskeleton without compensatory up-regulation of ezrin or radixin in moesin gene knockout. J. Biol. Chem. 274 (4), 2315–2321.

Dumonceaux, J., Nisole, S., Chanel, C., Quivet, L., Amara, A., Baleux, F., Briand, P., Hazan, U., 1998. Spontaneous mutations in the env gene of the human immunodeficiency virus type 1 NDK isolate are associated with a CD4-independent entry phenotype. J. Virol. 72 (1), 512–519.

Faure, S., Salazar-Fontana, L.I., Semichon, M., Tybulewicz, V.L., Bismuth, G., Trautmann, A., Germain, R.N., Delon, J., 2004. ERM proteins regulate cytoskeleton relaxation promoting T cell-APC conjugation. Nat. Immunol. 5 (3), 272–279.

Fievet, B., Louvard, D., Arpin, M., 2006. ERM proteins in epithelial cell organization and functions. Biochim. Biophys. Acta.

Gupta, N., Wollscheid, B., Watts, J.D., Scheer, B., Aebersold, R., DeFranco, A.L., 2006. Quantitative proteomic analysis of B cell lipid rafts reveals that ezrin regulates antigen receptor-mediated lipid raft dynamics. Nat. Immunol. 7 (6), 625–633.

Iwakuma, T., Cui, Y., Chang, L.J., 1999. Self-inactivating lentiviral vectors with U3 and U5 modifications. Virology 261 (1), 120–132.

Iyengar, S., Hildreth, J.E., Schwartz, D.H., 1998. Actin-dependent receptor colocalization required for human immunodeficiency virus entry into host cells. J. Virol. 72 (6), 5251–5255.

Jimenez-Baranda, S., Gomez-Mouton, C., Rojas, A., Martinez-Prats, L., Mira, E., Ana Lacalle, R., Valencia, A., Dimitrov, D.S., Viola, A., Delgado, R., Martinez, A.C., Manes, S., 2007. Filamin-A regulates actin-dependent clustering of HIV receptors. Nat. Cell Biol. 9 (7), 838–846.

Jolly, C., Kashefi, K., Hollinshead, M., Sattentau, Q.J., 2004. HIV-1 cell to cell transfer across an Env-induced, actin-dependent synapse. J. Exp. Med. 199 (2), 283–293.

Jolly, C., Sattentau, Q.J., 2005. Human immunodeficiency virus type 1 virological synapse formation in T cells requires lipid raft integrity. J. Virol. 79 (18), 12088–12094.

Kameoka, M., Kitagawa, Y., Utachee, P., Jinnopat, P., Dhepakson, P., Isarangkura-na-ayuthaya, P., Tokunaga, K., Sato, H., Komano, J., Yamamoto, N., Oguchi, S., Natori, Y., Ikuta, K., 2007. Identification of the suppressive factors for human immunodeficiency virus type-1 replication using the siRNA mini-library directed against host cellular genes. Biochem. Biophys. Res. Commun. 359 (3), 729–734.

Kikuchi, S., Hata, M., Fukumoto, K., Yamane, Y., Matsui, T., Tamura, A., Yonemura, S., Yamagishi, H., Keppler, D., Tsukita, S., Tsukita, S., 2002. Radixin deficiency causes conjugated hyperbilirubinemia with loss of Mrp2 from bile canalicular membranes. Nat. Genet. 31 (3), 320–325.

Kizhatil, K., Albritton, L.M., 1997. Requirements for different components of the host cell cytoskeleton distinguish ecotropic murine leukemia virus entry via endocytosis from entry via surface fusion. J. Virol. 71 (10), 7145–7156.

Kozak, S.L., Heard, J.M., Kabat, D., 2002. Segregation of CD4 and CXCR4 into distinct lipid microdomains in T lymphocytes suggests a mechanism for membrane destabilization by human immunodeficiency virus. J. Virol. 76 (4), 1802–1815.

Kubo, Y., Ishimoto, A., Amanuma, H., 2003. N-Linked glycosylation is required for XC cell-specific syncytium formation by the R peptide-containing envelope protein of ecotropic murine leukemia viruses. J. Virol. 77 (13), 7510–7516.

Kusagawa, S., Sato, H., Tomita, Y., Tatsumi, M., Kato, K., Motomura, K., Yang, R., Takebe, Y., 2002. Isolation and characterization of replication-competent molecular DNA clones of HIV type 1 CRF01_AE with different coreceptor usages. AIDS Res. Hum. Retrovir. 18 (2), 115–122.

Lehmann, M.J., Sherer, N.M., Marks, C.B., Pypaert, M., Mothes, W., 2005. Actin- and myosin-driven movement of viruses along filopodia precedes their entry into cells. J. Cell Biol. 170 (2), 317–325.

Naghavi, M.H., Valente, S., Hatziioannou, T., de Los Santos, K., Wen, Y., Mott, C., Gundersen, G.G., Goff, S.P., 2007. Moesin regulates stable microtubule formation and limits retroviral infection in cultured cells. EMBO J. 26 (1), 41–52.

Naldini, L., Blomer, U., Gallay, P., Ory, D., Mulligan, R., Gage, F.H., Verma, I.M., Trono, D., 1996. In vivo gene delivery and stable transduction of nondividing cells by a lentiviral vector. Science 272 (5259), 263–267.

Nguyen, D.H., Giri, B., Collins, G., Taub, D.D., 2005. Dynamic reorganization of chemokine receptors, cholesterol, lipid rafts, and adhesion molecules to sites of CD4 engagement. Exp. Cell Res. 304 (2), 559–569.

Platt, E.J., Wehrly, K., Kuhmann, S.E., Chesebro, B., Kabat, D., 1998. Effects of CCR5 and CD4 cell surface concentrations on infections by macrophagetropic isolates of human immunodeficiency virus type 1. J. Virol. 72 (4), 2855–2864.

Pontow, S.E., Heyden, N.V., Wei, S., Ratner, L., 2004. Actin cytoskeletal reorganizations and coreceptor-mediated activation of rac during human immunodeficiency virus-induced cell fusion. J. Virol. 78 (13), 7138–7147.

Rana, T.M., 2007. Illuminating the silence: understanding the structure and function of small RNAs. Nat. Rev., Mol. Cell Biol. 8 (1), 23–36.

Roumier, A., Olivo-Marin, J.C., Arpin, M., Michel, F., Martin, M., Mangeat, P., Acuto, O., Dautry-Varsat, A., Alcover, A., 2001. The membrane-microfilament linker ezrin is involved in the formation of the immunological synapse and in T cell activation. Immunity 15 (5), 715–728.

Saotome, I., Curto, M., McClatchey, A.I., 2004. Ezrin is essential for epithelial organization and villus morphogenesis in the developing intestine. Dev. Cell 6 (6), 855–864.

Steffens, C.M., Hope, T.J., 2003. Localization of CD4 and CCR5 in living cells. J. Virol. 77 (8), 4985–4991.

Steffens, C.M., Hope, T.J., 2004. Mobility of the human immunodeficiency virus (HIV) receptor CD4 and coreceptor CCR5 in living cells: implications for HIV fusion and entry events. J. Virol. 78 (17), 9573–9578.

Takeuchi, K., Sato, N., Kasahara, H., Funayama, N., Nagafuchi, A., Yonemura, S., Tsukita, S., Tsukita, S., 1994. Perturbation of cell adhesion and microvilli formation by antisense oligonucleotides to ERM family members. J. Cell Biol. 125 (6), 1371–1384.

Tanaka, R., Yoshida, A., Murakami, T., Baba, E., Lichtenfeld, J., Omori, T., Kimura, T., Tsurutani, N., Fujii, N., Wang, Z.X., Peiper, S.C., Yamamoto, N., Tanaka, Y., 2001. Unique monoclonal antibody recognizing the third extracellular loop of CXCR4 induces lymphocyte agglutination and enhances human immunodeficiency virus type 1-mediated syncytium formation and productive infection. J. Virol. 75 (23), 11534–11543.

Tsukita, S., Yonemura, S., Tsukita, S., 1997. ERM proteins: head-to-tail regulation of actin–plasma membrane interaction. Trends Biochem. Sci. 22 (2), 53–58.

Viard, M., Parolini, I., Sargiacomo, M., Fecchi, K., Ramoni, C., Ablan, S., Ruscetti, F.W., Wang, J.M., Blumenthal, R., 2002. Role of cholesterol in human immunodeficiency virus type 1 envelope protein-mediated fusion with host cells. J. Virol. 76 (22), 11584–11595.

Yokomaku, Y., Miura, H., Tomiyama, H., Kawana-Tachikawa, A., Takiguchi, M., Kojima, A., Nagai, Y., Iwamoto, A., Matsuda, Z., Ariyoshi, K., 2004. Impaired processing and presentation of cytotoxic-T-lymphocyte (CTL) epitopes are major escape mechanisms from CTL immune pressure in human immunodeficiency virus type 1 infection. J. Virol. 78 (3), 1324–1332.

AIDS RESEARCH AND HUMAN RETROVIRUSES
Volume 24, Number 3, 2008

DOI: 10.1089/aid.2007.0092

# Enhancement of OX40-Induced Apoptosis by TNF Coactivation in OX40-Expressing T Cell Lines *in Vitro* Leading to Decreased Targets for HIV Type 1 Production

YOSHIAKI TAKAHASHI,[1,*] REIKO TANAKA,[1] NAOKI YAMAMOTO,[2] and YUETSU TANAKA[1]

## ABSTRACT

**OX40, a member of the tumor necrosis factor receptor (TNF-R) superfamily, has been shown to play an important role in the survival of antigen-specific CD4$^+$ T cells. We have previously reported that stimulation of the OX40-expressing and HIV-1 chronically infected T cell line, ACH-2/OX40, with either OX40 ligand (OX40L)-expressing cells or with TNF resulted in the activation of HIV-1 followed by apoptotic cell death. In the present study we found that costimulation via OX40 and TNF-R in OX40-expressing HIV-1-infected T cell lines leads to a marked reduction of HIV-1 production associated with rapid cell death. Since HIV-1-negative OX40$^+$ T cell lines underwent rapid apoptotic cell death after OX40L and TNF stimulation, it was reasoned that the ACH-2/OX40 cell death was unlikely to be due to HIV-1 infection. Furthermore, we found that the OX40-mediated apoptosis of the CD4$^+$ T cell line, Molt-4/CCR5-OX40 (M/R5-OX40), required (1) signals mediated via the cytoplasmic tail of OX40, (2) activation of the caspase cascade, including caspase-8 and caspase-3, and (3) induction of endogenous TNF-$\alpha$, but not of TNF-$\beta$, FasL, or TNF-related apoptosis-inducing ligand (TRAIL), suggesting that this apoptosis occurred indirectly via the TNF/TNF-R system. Finally, a fraction of primary activated CD4$^+$ T cells, expressing high levels of OX40, underwent apoptosis, as revealed by annexin V staining, after cocultivation with OX40L$^+$ cells. These results suggest a new biological role of the OX40L/OX40 system in controlling the fate of activated CD4$^+$ T cells and of controlling HIV-1 infection in inflammatory environments.**

## INTRODUCTION

OX40 (CD134) is a 50-kDa transmembrane protein that serves as a marker of activated T cells. It is a member of the tumor necrosis factor receptor (TNF-R) superfamily, a family that also includes TNF-R1, TNF-R2, CD30, CD40, CD27, CD95 (Fas), TNF-related apoptosis-inducing ligand receptor (TRAIL-R) 1, and TRAIL-R2.[1–3] Its ligand, in humans, OX40L (CD252), was originally identified on human T cell leukemia virus type-1 (HTLV-I)-infected T cell lines and was termed gp34.[4,5] OX40L belongs to the tumor necrosis factor (TNF) superfamily[6] and is expressed predominantly on normal activated dendritic cells (DCs),[7] B cells,[8,9] vein endothelial cells,[10] and stimulated monocytes.[11] OX40-mediated costimulation of CD4$^+$ T cells by OX40L induces nuclear factor-kappa B (NF-$\kappa$B) activation through TNF-R-associated factor (TRAF)2 and TRAF5,[12] and is associated with a number of immune function activities. These include the enhanced synthesis of T helper (Th) 2 responses from naive CD4$^+$ T cells,[13–15] the production of both Th1 and Th2 cytokines,[16–18] the development and survival of memory CD4$^+$ T cells,[17] the prevention of peripheral CD4$^+$ T cell tolerance,[19] and the ability to block the inhibitory activity of CD4$^+$ CD25$^+$ T regulatory cells.[20] Ligation of OX40L on activated B cells and on immature DC, *in vitro*, results in enhanced immunoglobulin production[9] and maturation of DC,[7] respectively. In addition to these costimulatory functions, additional OX40/OX40L functions include not only the promotion of cell-to-cell adhesion between activated or HTLV-I$^+$ leukemic CD4$^+$ T cells and OX40L$^+$ vein endothelial cells,[21] but also the migration of CD4$^+$ T cells to B cell follicles in pe-

[1]Department of Immunology, Graduate School of Medicine, University of the Ryukyus, Okinawa 903-0215, Japan.
[2]AIDS Research Center, National Institute of Infectious Diseases, Tokyo 162-8640, Japan.
*Present address: AIDS Research Center, National Institute of Infectious Diseases, Tokyo 162-8640, Japan.

ripheral lymph nodes.[22] The failure to properly control OX40/OX40L interaction has been suggested to cause immune abnormalities such as autoimmune diseases,[23–25] allergy,[26,27] or defective protection against pathogens.[15,28–30]

In addition to its ability to induce cell activation, the TNF-R superfamily is also associated with promoting cell death. One group of the TNF-R superfamily, consisting of Fas, TNF-R1, TRAIL-R1, and TRAIL-R2, mediates cell death through their intracytoplasmic death domain (DD). A second group, consisting of the DD-lacking receptors, TNF-R2, CD27, CD30, CD40, 4-1BB, and OX40, is capable of inducing cell death under certain conditions. Thus, for example, activation of TNF-R2 triggers apoptosis of a rhabdomyosarcoma cell line and of HeLa cells.[31] The activation of CD27 induces apoptosis of B cell lines[32] and the activation of CD30 by specific antibody mediates apoptosis of an anaplastic large cell lymphoma[33] and of a T cell hybridoma costimulated with anti-T cell receptor (TCR).[34] In addition, the activation of CD40 by antibody induces apoptosis in transformed cell lines and in normal activated $CD4^+$ T cells costimulated with anti-CD3 antibody.[31,35] The precise mechanisms of cell death induced by the DD-lacking TNF-R superfamily remain to be elucidated. Recently, it has been shown that TNF-R2 stimulation causes TNF-R1-dependent apoptosis by the depletion of the antiapoptotic proteins TRAF2 and IAP.[36,37] We have previously shown that OX40 stimulation activates human immunodeficiency virus type-1 (HIV-1) production in the chronically HIV-1-infected T cell line ACH-2/OX40 through the activation of NF-$\kappa$B.[38] This mechanism is consistent with another member of the TNF-R superfamily, CD30.[39] Following stimulation with either OX40L or TNF, ACH-2/OX40 cells undergo not only HIV-1 activation but also apoptotic cell death within 48 h.[38]

In the present study, we examined the fate of cells following either OX40 stimulation alone or stimulation with OX40 in combination with TNF. Surprisingly, costimulation resulted in a marked decrease of HIV-1 production, as a consequence of rapid cell death of the T cell line. The cell death was reasoned not to be secondary to HIV-1 infection since OX40 stimulation alone and/or costimulation with TNF also induced cell death of HIV-1-negative T cell lines. Furthermore, the cell death in the T cell lines via OX40 stimulation was mediated indirectly by the TNF/TNF-R system. These observations suggest a new immunological role of OX40.

## MATERIALS AND METHODS

### *Reagents*

The medium used consisted of RPMI 1640 medium (Sigma, St. Louis, MO), supplemented with 10% fetal calf serum (FCS; Sigma), 100 U/ml of penicillin, and 100 $\mu$g/ml of streptomycin (hereinafter called RPMI medium). Antihuman (h) CD3 (clone OKT-3) and anti-hCD4 (clone OKT-4) monoclonal antibodies (mAbs) were purchased from the American Type Culture Collection (Rockville, MD). Anti-hOX40 mAb (clone B-17D8; mouse IgG2b, $\kappa$) was newly generated by a previously described method.[38] Anti-hTNF-$\alpha$, anti-hTNF-$\beta$, and anti-hTRAIL mAbs, for neutralization, were purchased from R&D (Minneapolis, MN). Anti-hFasL neutralizing mAb was purchased from BD Pharmingen (San Diego, CA). Anti-hCaspase-8 and anti-hCaspase-3 mAbs were purchased from Cell Signaling (Danvers, MA) and horseradish peroxidase (HRPO)-conjugated goat antimouse immunoglobulin G (IgG) Ab was purchased from Chemicon (Temecula, CA). Anti-hOX40L neutralizing mAb (clone 5A8)[40] and isotype control mouse IgG1 (mIgG1), anti-HTLV-I Tax mAb (clone TAXY-8),[41] have been described previously. Isotype control mIgG2a and mIgG2b were purchased from BD Pharmingen and ImmunoTools (Friesoythe, Germany), respectively. Recombinant human TNF-$\alpha$ (rhTNF-$\alpha$), TNF-$\alpha$ (rhTNF-$\beta$), interleukin-4 (rhIL-4), and rhIL-12 were purchased from Peprotec (London, UK). rhIL-2 was purchased from Shionogi Pharmaceutical (Osaka, Japan). The broad-spectrum caspase inhibitor, z-VAD-fmk, was purchased from MBL (Nagoya, Japan), dissolved in dimethyl sulfoxide and diluted in medium prior to use. Apoptosis was assessed by the annexin V-fluorescein isothiocyanate (FITC)/propidium iodide (PI) staining kit (Sigma and R&D). The hTNF-$\alpha$ sandwich enzyme-linked immunosorbent assay (ELISA) kit was purchased from R&D. The advanced protein assay reagent was purchased from Cytoskeleton (Denver, CO).

### *Cells*

The hOX40-transfected and the HIV-1 chronically infected human T cell line cells, ACH-2/OX40 (cell groups 4 and 10), and its vector control, ACH-2/control (mock), and the hOX40L-tranfected mouse SV-T2 cell line, SV-T2/OX40L (gp34), and its vector control, SV-T2/control (mock), have been previously described.[38] The cell lines utilized for transfections of OX40, OX40L, and control vector were the human T cell lines Molt-4/CCR5[42] [Molt-4/CCR5-OX40 (M/R5-OX40), -OX40L, and -control], CEM (CEM/OX40, /OX40L, and /control), Jurkat (Jurkat/OX40, /OX40L, and /control), and HIV-1 productively infected human T cell line Molt-4/IIIB [Molt-4/IIIB-OX40 (M/IIIB-OX40), -OX40L, and -control], the human promonocytic cell lines U937 (U937/OX40, /OX40L, and /control), THP-1 (THP-1/OX40, /OX40L, and /control), and HIV-1 chronically infected human promonocytic cell line U1 (U1/OX40, /OX40L, and /control), and the human B cell line BJAB (BJAB/OX40, /OX40L, and /control). Aliquots of each of these cell lines were transfected by electroporation of 10–15 $\mu$g of the individual plasmids, pCAGIPuro/OX40, pCAGIPuro/OX40L, and control pCAGIPuro, as previously described.[38] In addition, the Molt-4/CCR5 cell line was also transfected with an expression vector containing the OX40 cytoplasmic tail-deleted mutant, pCAGIPuro/OX40-del(6-725), constructed as previously described,[38] to generate Molt-4/CCR5-OX40del cells. For the selection of transfectants, 1 $\mu$g/ml puromycin (Wako, Osaka, Japan) was added to the culture media. Expression of OX40 or OX40L in selectively grown cells was determined by flow cytometric analysis, as previously described.[38]

### *Detection of cell death and apoptosis*

SV-T2/OX40L and SV-T2/control stimulator cells were fixed with 4% paraformaldehyde (PFA) for 15 min and washed three times in phosphate-buffered saline (PBS) prior to use. The OX40-expressing responder cells, at $4 \times 10^5$ cells/ml, were cocultured with various ratios of PFA-fixed stimulator cells in RPMI medium in the presence or absence of rhTNF-$\alpha$ (2 ng/ml)

or in the presence or absence of rhTNF-$\beta$ (10 ng/ml) in 48-well culture plates (0.5 ml/well). The cocultures were incubated overnight, or for the indicated periods, at 37°C in 5% $CO_2$ humidified atmosphere. For blocking of the OX40–OX40L interaction, anti-hOX40L mAb (5A8) was added at a final concentration of 10–40 $\mu$g/ml at 37°C for 1 h prior to coculture. In some cases, anti-hTNF-$\alpha$, anti-hTNF-$\beta$, anti-hTRAIL, and anti-hFasL blocking mAbs were added at a final concentration of 30–100 $\mu$g/ml at 37°C for 1 h prior to coculture. For inhibition of the caspase-dependent pathways of apoptosis, z-VAD-fmk was included in the culture medium at concentrations of 100 $\mu$M. The viability of the responder cells was determined, in triplicate, using a hemocytometer after staining with 0.1% eosin-Y (Wako, Osaka, Japan). The eosin-Y-stained PFA-fixed stimulator SV-T2/OX40L or SV-T2/control cells could be easily distinguished from dead responder cells by their distinct morphology. Apoptotic and necrotic cells were detected by staining with annexin V-FITC and PI, according to the manufacturer's instructions, utilizing a FACSCalibur (Becton Dickinson, San Jose, CA). The data obtained were analyzed using CellQuest software (Becton Dickinson).

### *HIV-1 production assay*

Production of HIV-1 was determined by the measurement of HIV-1 core p24 levels using a commercial ELISA kit (ZeptoMetrix Corporation, Buffalo, NY). Data were analyzed by the Student's *t*-test. To examine the effect of OX40L and/or TNF stimulation on HIV-1 acutely infected T cell lines, M/R5-OX40 and M/R5-control were infected with the HIV-1 molecular clone NL4-3[43] at a multiplicity of infection (MOI) of 0.01 in 0.1 ml for 3 h at 37°C, as previously described.[44] The infected cells were subsequently washed twice and cultured at $2 \times 10^5$ cells/ml for 24 h in 48-well culture plates (0.5 ml/well). The infected cells were cocultured with PFA-fixed SV-T2/OX40L or with PFA-fixed SV-T2/control cells at a cell-to-cell ratio of 2:1 in the presence or in the absence of rhTNF-$\alpha$ (2 ng/ml), for an additional 3 days. Cell-free supernatant fluid was collected and the levels of p24 were quantified.

### *Western blotting*

Western blot analysis was performed as previously described.[38] Briefly, M/R5-OX40 cells ($4 \times 10^5$ cells/well) were stimulated by PFA-fixed SV-T2/OX40L or by PFA-fixed SV-T2/control cells ($2 \times 10^5$ cells/well) for 6 h in 12-well plates. Cell lysates were obtained by lysis of $2.5–4 \times 10^7$ cells in 1 ml of a lysis buffer (10 mM Tris–HCl, pH 8.0, 140 mM NaCl, 3 mM $MgCl_2$, 2 mM phenylmethylsulfonyl fluoride, 0.5% Nonidet P-40) on ice for 20 min, followed by centrifugation at $13,000 \times g$ for 10 min at 4°C. The cell lysates (6 $\mu$g protein/lane) were treated with an equal volume of 2× sample buffer [125 mM Tris–HCl, pH 6.8, 4% sodium dodecyl sulfate (SDS), 20% glycerol, 0.1% bromophenol blue] without 2-mercaptoethanol, separated by SDS–polyacrylamide gel electrophoresis (PAGE), using a 12.5% gel, and then transferred to Immobilon-P Transfer Membrane (Millipore, Bedford, MA). The membrane was blocked with a blocking buffer [1% bovine serum albumin (BSA) in PBS] at 4°C overnight and incubated with the primary anti-hCaspase-8 and anti-hCaspase-3 mAbs (1:1000) according to the manufacturer's instructions. Mem-

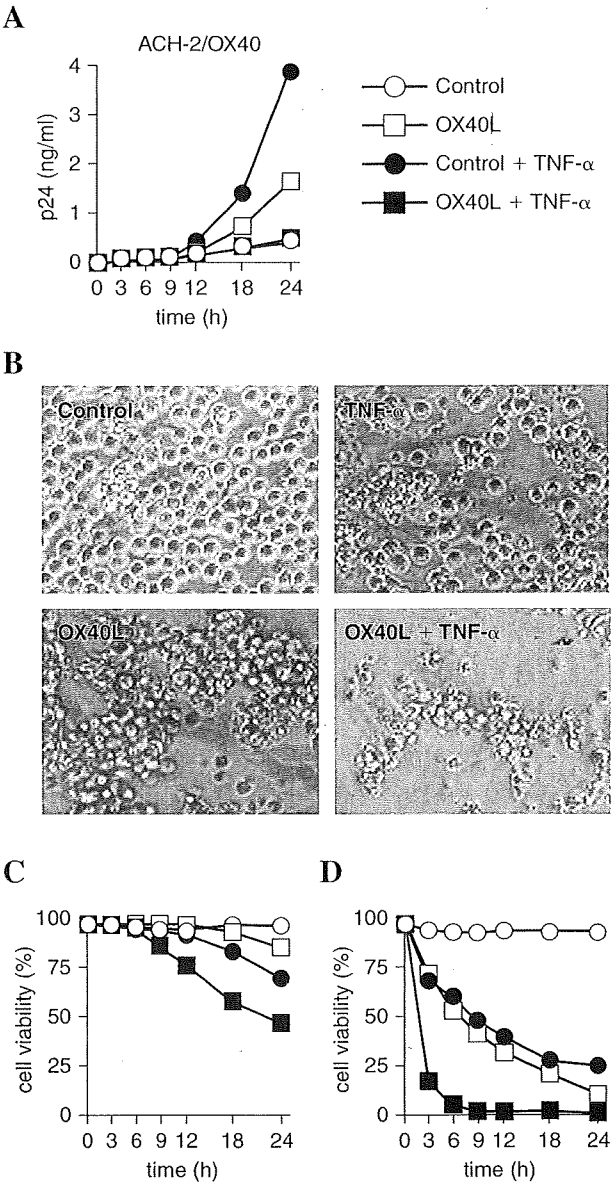


**FIG. 1.** Marked reduction of HIV-1 production and induction of rapid apoptosis by dual stimulation of ACH-2/OX40 cells with OX40L and TNF. ACH-2/OX40 cells (cell group 10) were cocultured with PFA-fixed SV-T2/OX40L (OX40L) or with PFA-fixed SV-T2/control (Control) cells in the presence or in the absence of TNF-$\alpha$ at 2 ng/ml for 24 h. (**A**) The kinetics of HIV-1 production, as determined by the level of HIV-1 p24 in the culture supernatants, (**B**) microscopic observation of morphological changes, (**C**) the kinetics of cell death as determined by an eosin-Y dye exclusion assay, and (**D**) the kinetics of apoptosis as determined by annexin V/PI staining. Morphological changes were examined under an inverted microscope at 100× original magnification. The cell viability was shown as percentage of control. Representative results from three independent experiments are shown. The data presented are the mean values ± SD of triplicate determinations.

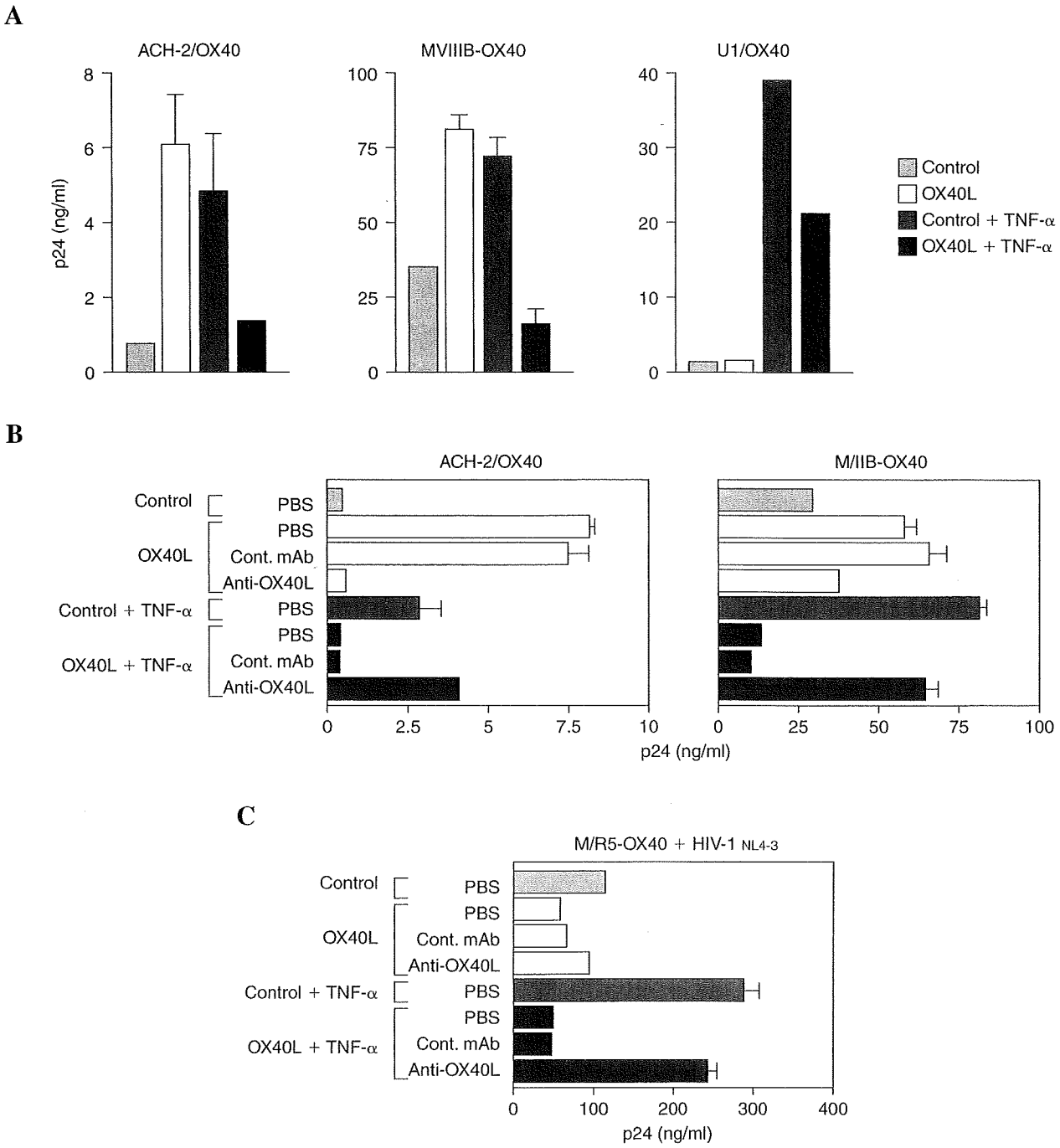


**FIG. 2.** Reduction of HIV-1 production in various HIV-1-infected cell lines. Several OX40-expressing cell lines were cocultured with PFA-fixed SV-T2/OX40L (OX40L) or with PFA-fixed SV-T2/control (Control) cells in the presence or absence of TNF-$\alpha$ (2 ng/ml) for 24 h. The levels of HIV-1 p24 produced in the culture supernatants were determined by ELISA. (**A**) Representative data was obtained using the HIV-1 chronically infected ACH-2/OX40 cells (cell group 4), the HIV-1 productively infected Molt-4/IIIB-OX40 cells (M/IIIB-OX40), and the HIV-1 chronically infected U1/OX40 cells. (**B**) The blocking effect of the anti-OX40L mAb (Anti-OX40L, 10 $\mu$g/ml for ACH-2/OX40 and 40 $\mu$g/ml for M/IIIB-OX40), negative control mAb (Cont. mAb, the same conditions as above) or of PBS was determined using ACH-2/OX40 and M/IIIB-OX40 cells. (**C**) The Molt-4/CCR5-OX40 cells (M/R5-OX40) were acutely infected with HIV-$1_{NL4-3}$ at an MOI of 0.01, were precultured for 24 h, and were stimulated with OX40L and/or with TNF for an additional 72 h. The blocking effect of equal volumes of anti-OX40L mAb (Anti-OX40L, 10 $\mu$g/ml), negative control mAb (Cont. mAb, 10 $\mu$g/ml), or of PBS was determined. The data presented are the mean values ± SD of triplicate determinations. Representative results from three independent experiments are shown.

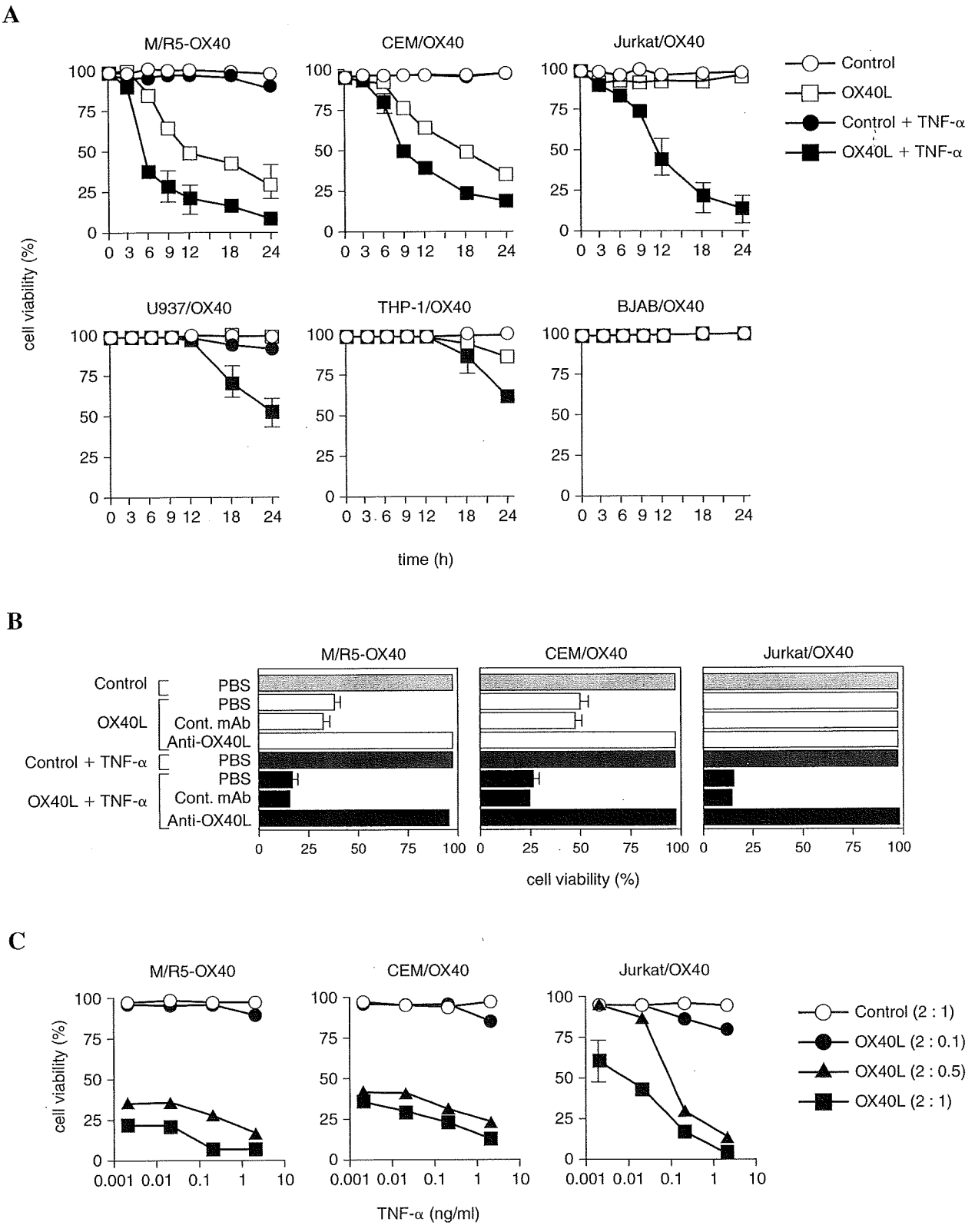


**FIG. 3.** Cell type-dependent induction of cell death by stimulation with OX40L alone or by combined activation with OX40L and TNF. Cell viability was determined by an eosin-Y dye exclusion assay, 24 h after stimulation by coculture with PFA-fixed SV-T2/OX40L (OX40L) or with PFA-fixed SV-T2/control (Control) cells in the presence or absence of TNF-$\alpha$ (2 ng/ml or graded concentrations). (**A**) The three CD4$^+$ T cell lines, Molt-4/CCR5-OX40 (M/R5-OX40), CEM/OX40, and Jurkat/OX40, the two promonocytic cell lines U937/OX40 and THP-1/OX40, and the B cell lines BJAB/OX40 were examined. (**B**) The blocking effect of anti-hOX40L mAb (Anti-OX40L, 10 $\mu$g/ml) on cell death of OX40-expressing CD4$^+$ T cell lines was determined. (**C**) The cell death of OX40-expressing CD4$^+$ T cell lines was induced by the addition of various concentrations of TNF-$\alpha$, up to 2 ng/ml, and by various ratios of stimulator to responder cell. Data presented are the mean values ± SD of triplicate determinations. Representative results from three independent experiments are shown.

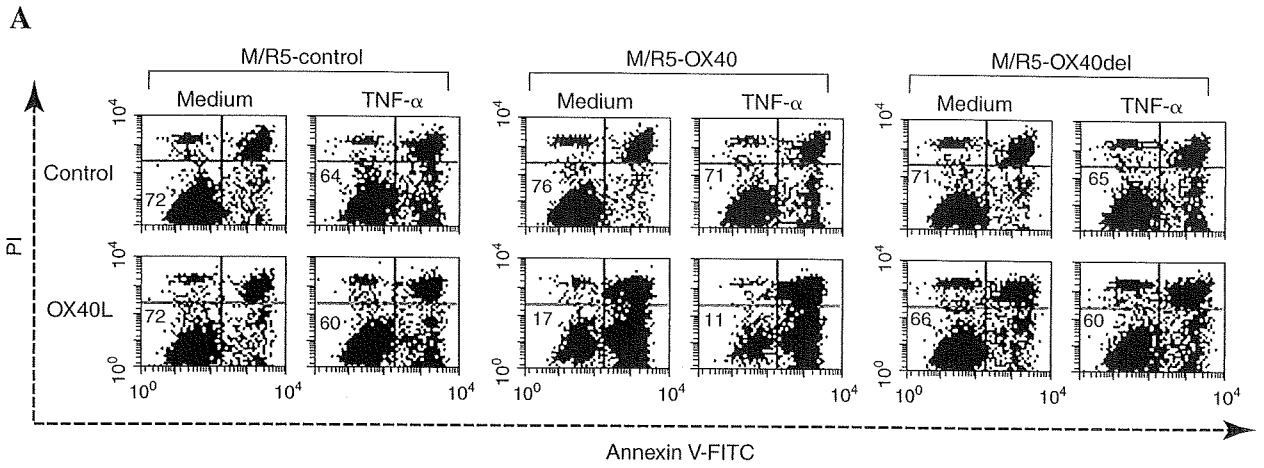
A
M/R5-control
M/R5-OX40
M/R5-OX40del
Medium
TNF-α
Control
OX40L
PI
Annexin V-FITC
72
64
76
71
71
65
72
60
17
11
66
60

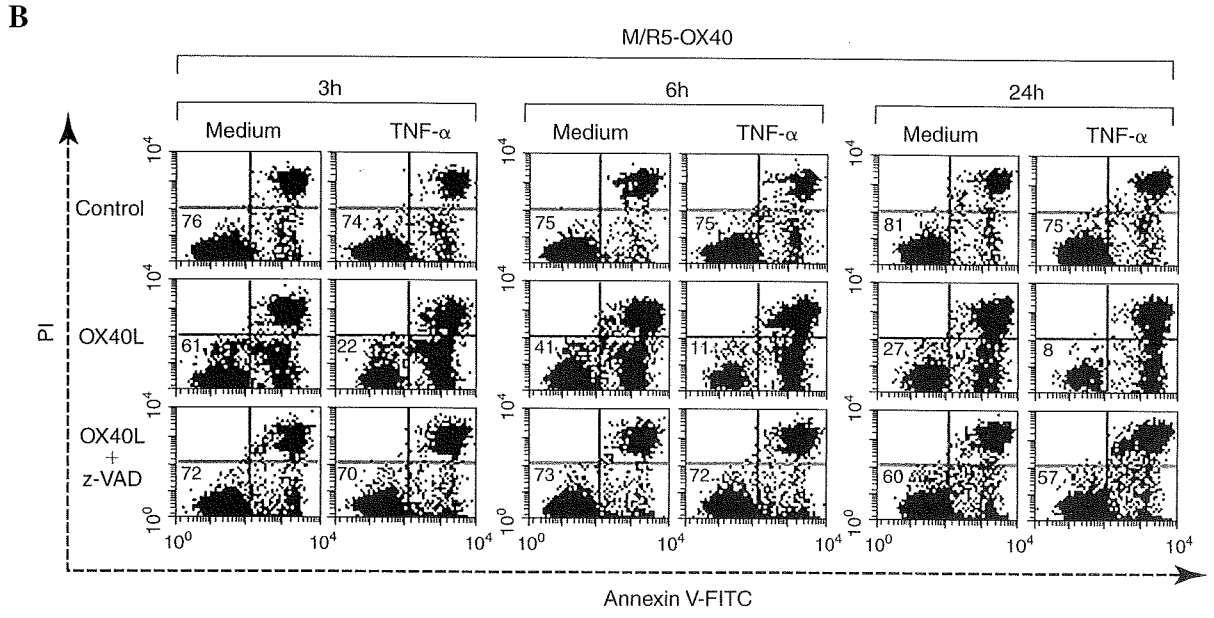
B
M/R5-OX40
3h
6h
24h
Medium
TNF-α
Control
OX40L
OX40L + z-VAD
PI
Annexin V-FITC
76
74
75
75
81
75
61
22
41
11
27
8
72
70
73
72
60
57

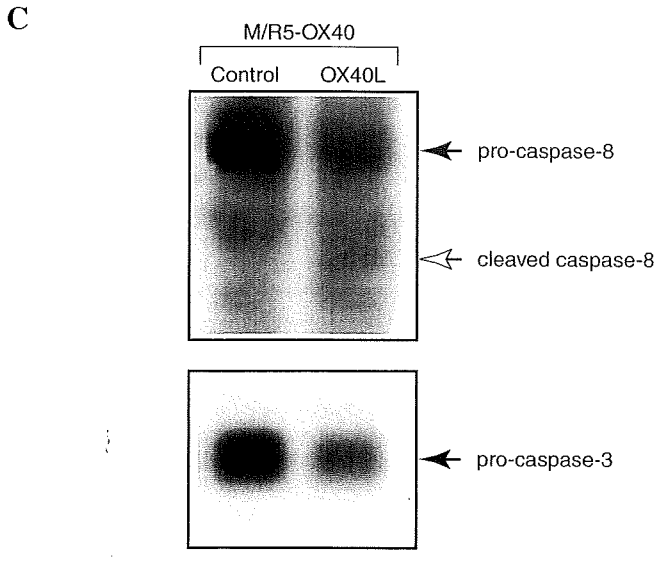
C
M/R5-OX40
Control
OX40L
pro-caspase-8
cleaved caspase-8
pro-caspase-3

branes were then incubated with HRPO-conjugated antimouse IgG Ab (1:2000). Signals were detected using Super Signal West Femto Maximum Sensitivity Substrate (Pierce, Rockford, IL) and the LAS-3000 image analyzer (Fujifilm, Tokyo, Japan).

### *TNF-α assay*

As described above, cells ($4 \times 10^5$ cells/well) were stimulated by PFA-fixed SV-T2/OX40L or by PFA-fixed SV-T2/control cells ($2 \times 10^5$ cells/well), for the times indicated, in 12-well plates. For the determination of TNF-α production, culture supernatants and cell lysates ($5\text{-}6 \times 10^6$ cells/ml) were collected, and the concentrations of TNF-α were assayed using the Quantikine human TNF-α kit (R&D). The protein concentrations in cell lysates were determined using the advanced protein assay reagent.

### *Detections of apoptosis in primary T cells*

Human peripheral blood mononuclear cells (PBMCs) were isolated from heparinized (5 U/ml) blood of normal healthy donors using standard density gradient centrifugation and a human lymphocyte separation medium (Sigma). The cells at the interface were collected and washed three times in PBS containing 2% FCS. PBMCs were resuspended at $1 \times 10^6$ cells/ml in RPMI medium, supplemented with 20 U/ml rhIL-2. Each well of 12-well plates was coated with 5 μg/ml anti-hCD3 mAb (clone OKT-3) for 1 h at 37°C and washed three times in PBS. Then, 1 ml of the cell suspension was dispensed into individual wells and cultured in the presence of either rhIL-12 or rhIL-4 at 20 ng/ml for 3 days at 37°C in a 5% $CO_2$ humidified incubator. The activated cells were harvested, adjusted to $2 \times 10^5$ cells/ml, and further stimulated using the same conditions at days 3 and 6. Activated PBMCs were harvested on day 9, in 20 U/ml rhIL-2-containing RPMI medium, and were then cocultivated for 24 h with either PFA-fixed SV-T2/OX40L or with PFA-fixed SV-T2/control cells at a cell to cell ratio of 1:1. Anti-hOX40L mAb (5A8) was added at 20 μg/ml to prevent OX40–OX40L interaction. The cells were then stained by Cy5-labeled anti-hCD4 mAb (OKT-4) followed by FITC-labeled annexin V to detect apoptosis. Apoptotic cells in the $CD4^+$ T cell gate were detected by FACSCalibur.

## RESULTS

### *Combined stimulation of ACH-2/OX40 cell line cells with OX40L and TNF decreases HIV-1 production by inducing rapid apoptosis*

We have previously reported that the chronically HIV-1-infected cell line ACH-2/OX40 produces large amounts of HIV-1 within 24 h, following stimulation by either coculture with OX40L-expressing cells or by the addition of TNF-α or -β. Such activation of HIV-1 replication is mediated primarily through activation of the NF-κB pathway.[38] In the present study, we examined the effect of dual stimulation by OX40L and TNF-α (or TNF-β, data not shown) on HIV-1 production. In contrast to the previously documented increase in HIV-1 production by activation via the ligation of either OX40 or TNF-R alone, dual stimulation of these two receptors resulted in a marked reduction of HIV-1 production in ACH-2/OX40 cells (Fig. 1A). The morphology of the ACH-2/OX40 cells was markedly altered following 24 h of dual stimulation (Fig. 1B). This morphological effect was associated with the induction of rapid apoptosis, as determined by apparent cell death (Fig. 1C) and by annexin V-FITC/PI staining (Fig. 1D). Of interest was the finding that all the dual receptor-stimulated ACH-2/OX40 cells became apoptotic as early as 9 h after stimulation, before HIV-1 production was detectable (Fig. 1A and D).

### *Dual receptor-induced activation also affects HIV-1 production in other HIV-1-infected cell line cells*

To determine whether this HIV-1 reduction and this rapid cell death, induced by such dual receptor activation, were unique to the ACH-2/OX40 cells or whether they are general for all types of HIV-1-infected cells expressing these two receptors, a series of other HIV-1 productively or chronically in-

**FIG. 4.** Involvement of the OX40 cytoplasmic tail and of the caspase cascade in the induction of apoptosis of Molt-4/CCR5-OX40 cells. (**A**) Molt-4/CCR5-OX40 (M/R5-OX40), Molt-4/CCR5-OX40del (M/R5-OX40del), and Molt-4/CCR5-control (M/R5-control) cells were cocultured with PFA-fixed SV-T2/OX40L (OX40L) or with PFA-fixed SV-T2/control (Control) cells, at a cell-to-cell ratio of 2:1 in the absence (Medium) or in the presence of 2 ng/ml TNF-α for 24 h. (**B**) The blocking of apoptosis of the M/R5-OX40 cells, induced by OX40L or by OX40L/TNF-α stimulation, by a caspase inhibitor, z-VAD-fmk. The caspase inhibitor z-VAD-fmk (z-VAD) was added, before stimulation, to M/R5-OX40 cells at a final concentration of 100 μM. The pretreated M/R5-OX40 cells were cocultured with PFA-fixed SV-T2/OX40L (OX40L) or with PFA-fixed SV-T2/control (Control) cells, at a cell-to-cell ratio of 2:1 in the absence (Medium) or in the presence of 2 ng/ml TNF-α for 3, 6, and 24 h. Apoptotic and live cells were determined by a standard dual staining method using annexin V-FITC and PI. The cells were classified as undamaged cells, annexin V(−)/PI(−); early apoptotic cells, annexin V(+)/PI(−); and late apoptotic cells and necrotic cells, annexin V(+)/PI(+). The stimulating cells, which included the PFA-fixed SV-T2/OX40L or SV-T2/control cells, were included within the region of annexin V(+)/PI(+) cells (about 20% of the total cell number). The percentage of live cells is shown at the lower left quadrangle of each dot plot. (**C**) The cell lysates obtained from the M/R5-OX40 cells stimulated by PFA-fixed SV-T2/OX40L (OX40L) or by PFA-fixed SV-T2/control (Control) cells, at a cell-to-cell ratio of 2:1 for 6 h, were treated with an equal volume of 2× sample buffer without 2-mercaptoethanol, separated by SDS–PAGE, using a 12.5% gel, and then transferred to Immobilon-P Transfer Membrane. After blocking, the membranes were incubated with the primary anticaspase-8 and anti-caspase-3 mAbs (1:1000) followed by horseradish peroxidase-conjugated antimouse IgG Ab (1:2000). The reaction was detected using Super Signal West Femto Maximum Sensitivity Substrate and an image analyzer. Representative results from three independent experiments are shown.

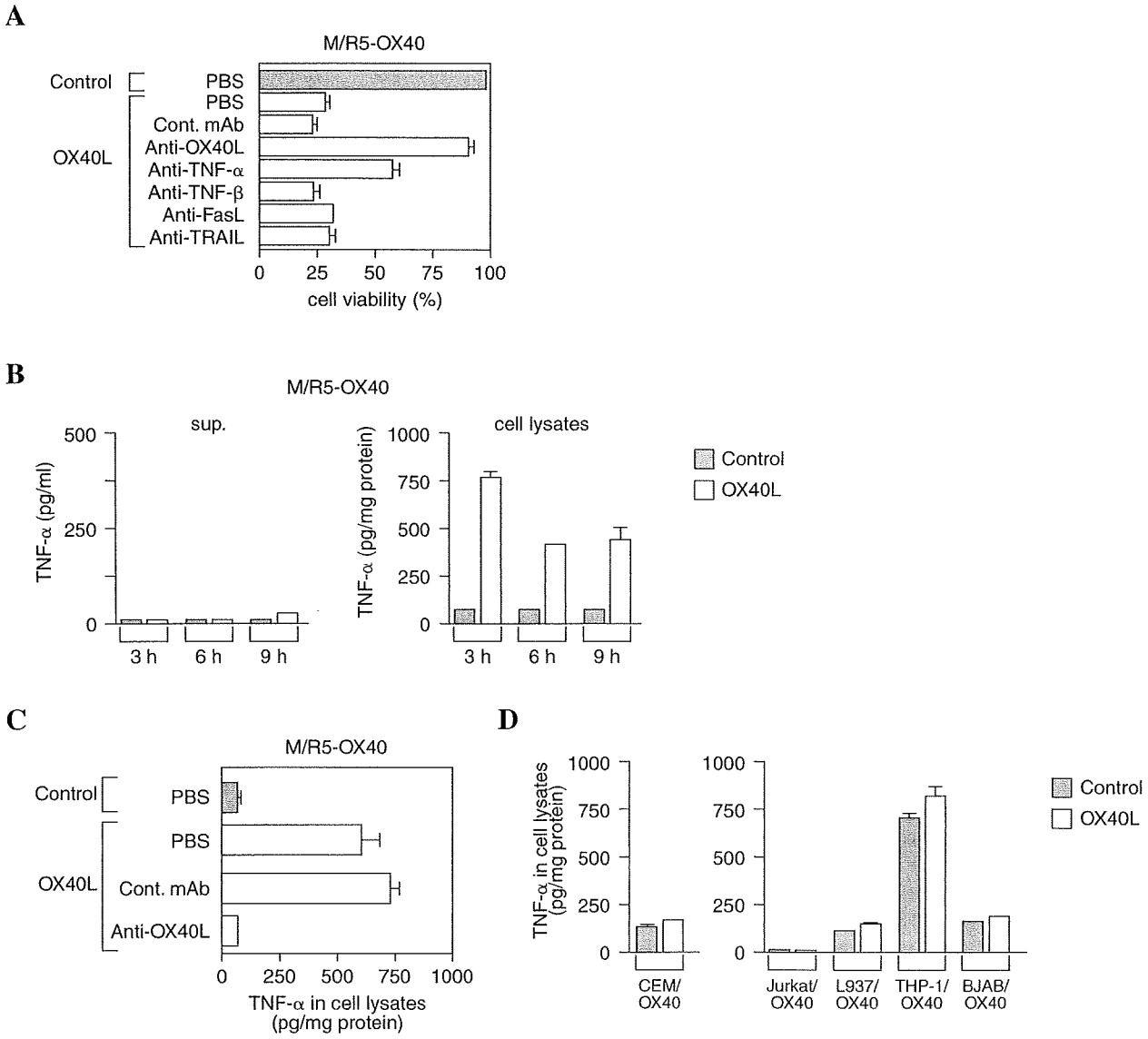


**FIG. 5.** OX40-induced apoptosis in Molt-4/CCR5-OX40 cells is mediated by endogenous TNF-$\alpha$. (**A**) Molt-4/CCR5-OX40 (M/R5-OX40) cells were stimulated by PFA-fixed SV-T2/OX40L (OX40L) or by PFA-fixed SV-T2/control (Conrol) cells in the presence or in the absence of anti-hTNF-$\alpha$ (Anti-TNF-$\alpha$, 30-100 $\mu$g/ml), anti-hTNF-$\beta$ (Anti-TNF-$\beta$, 100 $\mu$g/ml), anti-hTRAIL (Anti-TRAIL, 100 $\mu$g/ml), anti-hFasL (Anti-FasL, 100 $\mu$g/ml), and anti-hOX40L (Anti-OX40L, 10 $\mu$g/ml) neutralizing mAb or with isotype control (Cont. mAb) for 24 h. Live cells were determined by annexin V-FITC/PI staining, followed by FACS analysis. (**B**) M/R5-OX40 cells were stimulated for 3, 6, and 9 h by PFA-fixed SV-T2/OX40L (OX40L) or by PFA-fixed SV-T2/control (Control) cells. TNF-$\alpha$ concentrations were determined in the culture supernatants (sup., left panel) and in the cell lysates (cell lysates, right panel) by an hTNF-$\alpha$ sandwich ELISA. (**C**) M/R5-OX40 cells were stimulated by PFA-fixed SV-T2/OX40L (OX40L) or by PFA-fixed SV-T2/control (Control) cells in the presence or in the absence of anti-hOX40L neutralizing mAb (Anti-OX40L, 10 $\mu$g/ml) or with isotype control (Cont. mAb) for 6 h. TNF-$\alpha$ concentrations were determined in the cell lysates. (**D**) The cells were stimulated by PFA-fixed SV-T2/OX40L (OX40L) or by PFA-fixed SV-T2/control (Control) cells for 6 h, in the case of CEM/OX40 cells, and for 24 h in all other cells. TNF-$\alpha$ concentrations were determined in the culture supernatants and in the cell lysates. The data presented are the mean values $\pm$ SD of triplicate determinations. Representative results from three independent experiments are shown.

fected cell lines transfected with OX40 were examined. These cell lines included the OX40-transfected T cell line, Molt-4/IIIB, Molt-4/IIIB-OX40 (M/IIIB-OX40), and the promonocytic cell line, U1, U1/OX40. The M/IIIB-OX40 cells produced relatively large amounts of HIV-1 upon stimulation with either OX40L or with TNF-$\alpha$. The U1/OX40 cells produced significant levels of HIV-1 following stimulation with TNF-$\alpha$, but produced little following ligation using OX40L. On the other hand, dual receptor activation with OX40L and TNF-$\alpha$ dramatically reduced HIV-1 production in M/IIIB-OX40 and in U1/OX40 cells, similar to our findings using ACH-2/OX40 cells (Fig. 2A). In M/IIIB-OX40 cells, moderate cell death was observed following OX40L stimulation, while dual stimulation, with OX40L and TNF-$\alpha$, induced rapid cell death (data not

shown). In U1/OX40 cells, moderate cell death was induced only following dual stimulation (data not shown). The role of OX40/OX40L was underscored by the observation that antibody blockade of OX40L inhibited HIV-1 activation following OX40L stimulation. Antibody blockade also reversed HIV-1 reduction following dual stimulation with OX40L and TNF-$\alpha$ in ACH-2/OX40 and in M/IIIB-OX40 cells (Fig. 2B). Similarly, anti-OX40L blocking mAb partially or completely inhibited the cell deaths induced in ACH-2/OX40 and M/IIIB-OX40 cells following dual stimulation with OX40L and TNF-$\alpha$ (data not shown). The reduction of HIV-1 production resulting from dual receptor activation was also observed in the acutely HIV-1 NL4-3-infected Molt-4/CCR5-OX40 (M/R5-OX40) cells (Fig. 2C). This effect was also reversed by anti-OX40L blocking mAb. However, stimulation with OX40L alone did not enhance HIV-1 activation in acutely infected M/R5-OX40. The viability of the HIV-1 acutely infected M/R5-OX40 cells was rapidly reduced not only following dual stimulation with OX40L and TNF-$\alpha$ but also stimulation with OX40L alone as compared to ACH-2/OX40 and M/IIIB-OX40 cells (data not shown). This effect on cell viability was completely reversed with anti-OX40L blocking mAbs (data not shown). Therefore, these results support the view that OX40 stimulation by its natural ligand, OX40L, combined with stimulation by TNF-$\alpha$, leads to a significant reduction of HIV-1 production, which is associated with rapid cell death, not only in an ACH-2 cell line, but also in Molt-4/IIIB, U1, and HIV-1 acutely infected Molt-4/CCR5 cell lines.

### *OX40 ligation-mediated cell death occurs independently of HIV-1*

To determine whether the cell death of cells overexpressing OX40, induced by the stimulation with OX40L and/or TNF-$\alpha$, was intrinsic to the cytopathic effects of HIV-1 infection, we established a series of HIV-1-negative/OX40-positive and control vector transfectants. These cells were stimulated by coculture with OX40L$^+$ cells in the presence or absence of TNF-$\alpha$, followed by analysis of cell viability. As shown in Fig. 3A, cell death was seen in both the M/R5-OX40 and in the CEM/OX40 cells following stimulation by OX40L, and, furthermore, dual stimulation with OX40L and TNF-$\alpha$ synergistically accelerated the rate of cell death. In these two cell lines, TNF-$\alpha$ alone, at the doses utilized, had no effect on cell viability. On the other hand, in the case of another T cell line, Jurkat/OX40, and the two CD4$^+$ promonocytic cell lines, U937/OX40 and THP-1/OX40, dual receptor stimulation, but not OX40L stimulation alone, strongly induced cell death. However, the rate of cell death was more moderate in these cell lines than the rate observed with M/R5-OX40 and with CEM/OX40 cells. In contrast, the B cell line BJAB/OX40 was resistant to each of the stimulation protocols utilized above. As shown in Fig. 3B, death of OX40-expressing CD4$^+$ T cells, following stimulation with either OX40L or with OX40L and TNF-$\alpha$, was completely inhibited by anti-OX40L blocking mAb. This shows that OX40 triggering by OX40L was necessary for the induction of cell death. Maximum cell death was observed under close cell-to-cell contact between OX40$^+$ responder and OX40L$^+$ stimulator cells and at higher TNF-$\alpha$ concentrations (more than 2 ng/ml) (Fig. 3C). Therefore, in the absence of HIV-1, OX40-mediated signaling is capable, on its own, of inducing cell death, and the dual stimulation with OX40L and TNF-$\alpha$ leads to an accelerated rate of cell death than stimulation with either ligand alone, which differs with respect to the cell line being studied.

### *OX40-mediated apoptosis in M/R5-OX40 cells is induced by signaling via the cytoplasmic tail of OX40 and by the caspase cascade*

To confirm that the cell death, observed above, was dependent on signal transduction via OX40, we established a cell line expressing a deletion mutant of OX40 that lacked the cytoplasmic tail, Molt-4/CCR5-OX40del (M/R5-OX40del). M/R5-

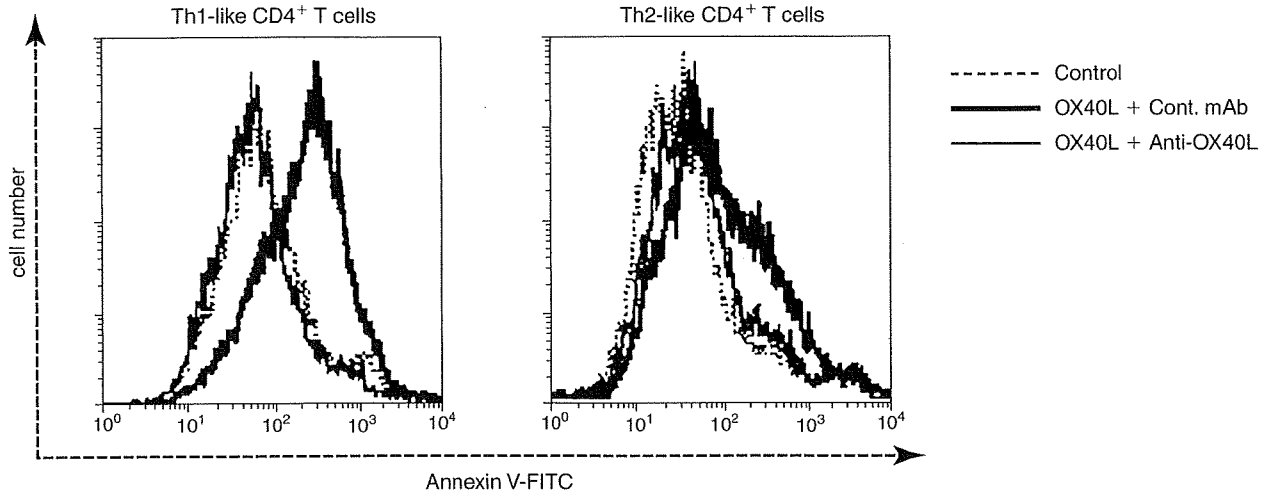


**FIG. 6.** Induction of apoptosis in primary activated CD4$^+$ T cells by cocultivation with OX40L-expressing cells. Two types of activated CD4$^+$ T cells from PBMCs of healthy donors, Th1-like and Th2-like, were activated in the presence of rhIL-12 and rhIL-4, respectively, on day 0, 3, and 6. After an additional 3 days, cells were cocultured with PFA-fixed SV-T2/OX40L (OX40L) or with PFA-fixed SV-T2/control (Control) cells in the presence of either anti-hOX40L blocking mAb (Anti-OX40L) or isotype control mAb (Cont. mAb). After 24 h, cells were stained by anti-hCD4-Cy5 and then stained by annexin V-FITC. Cells were analyzed with a FACSCalibur. Representative results from three independent experiments are shown.

OX40, M/R5-OX40del, and M/R5-control cells were stimulated with OX40L and/or TNF-$\alpha$, followed by the determination of cell viability using annexin V-FITC/PI staining. At 24 h following stimulation, apoptosis was apparent in M/R5-OX40 cells; however, no detectable apoptosis was observed in M/R5-OX40del cells (Fig. 4A), suggesting a signal from OX40 is indeed required for apoptosis. On the other hand, M/R5-OX40 cells pretreated with the broad-spectrum caspase inhibitor z-VAD-fmk and stimulated with OX40L, in the absence or presence of TNF-$\alpha$, were prevented from undergoing apoptosis (Fig. 4B), suggesting that the apoptosis was caspase cascade dependent. In accordance with this, Western blot assays showed that in OX40L-stimulated M/R5-OX40 cells, the levels of pre-caspase-8 (57 kDa) and pro-caspase-3 (32 kDa) were markedly reduced, and cleaved caspase-8 (43 kDa) was increased after OX40L stimulation (Fig. 4C). Taken together, these results indicate that the OX40-mediated apoptosis of M/R5-OX40 cells is dependent on both signaling via the cytoplasmic tail of OX40 and on the caspase cascade.

### *OX40-induced apoptosis in M/R5-OX40 cells is mediated by endogenous TNF-$\alpha$*

To explore the mechanisms involved in OX40-mediated apoptosis, M/R5-OX40 cells were examined in more detail, since these cells undergo apoptosis by OX40L stimulation without exogenous TNF. First, we examined the effects of various mAbs on OX40L-triggered cell death. As shown in Fig. 5A, anti-hTNF-$\alpha$ blocking mAb, but none of anti-hTNF-$\beta$, anti-hTRAIL, and anti-hFasL blocking mAbs, inhibited the cell death, showing that TNF-$\alpha$, but not TNF-$\beta$, TRAIL, and FasL, was involved in cell death after OX40L stimulation. Indeed, OX40L-stimulated M/R5-OX40 cells synthesized TNF-$\alpha$, which was detected in cell lysates, but not in culture supernatants (Fig. 5B). The fact that TNF-$\alpha$ was not detected in culture supernatants suggests that endogenously synthesized TNF-$\alpha$ bound to its membrane receptors (TNF-RI and/or TNF-RII) on the surface of cells stimulated with OX40L. The production of endogenous TNF-$\alpha$ was completely inhibited by anti-OX40L neutralizing mAb, showing that this endogenous TNF-$\alpha$ production was mediated by the OX40L/OX40 interaction (Fig. 5C). These results suggest that endogenous TNF-$\alpha$, induced by OX40 stimulation in the OX40$^+$ T cell line M/R5-OX40 mediates apoptosis. Furthermore, we also determined the induction of endogenous TNF-$\alpha$ in other OX40$^+$ cell lines. As shown in Fig. 5D, although endogenous TNF-$\alpha$ was induced in the T cell line CEM/OX40, it was not dependent on OX40L stimulation, unlike M/R5-OX40 cells. Interestingly, in another T cell line, Jurkat/OX40, endogenous TNF-$\alpha$ was not detected. On the other hand, two promonocytic cell lines, U937/OX40 and THP-1/OX40, strongly expressed endogenous TNF-$\alpha$ regardless of OX40 stimulation. The B cell line BJAB/OX40 also weakly expressed endogenous TNF-$\alpha$ regardless of OX40 stimulation. In all of these cell lines, soluble TNF-$\alpha$ was not detected in the culture supernatants after OX40L stimulation (data not shown).

### *Apoptosis of primary CD4$^+$ T cells by cocultivation with OX40L-expressing cells*

Finally, we determined whether apoptosis can be induced in primary CD4$^+$ T cells by OX40-stimulation *in vitro*. We generated two types of activated CD4$^+$ T cells from PBMCs of healthy donors, Th1-like and Th2-like, which were activated in the presence of IL-12 and IL-4, respectively. The Th1-like CD4$^+$ T cells expressed higher levels of functional OX40 than the Th2-like CD4$^+$ T cells.[45] These two types of cells were cocultured for 24 h with PFA-fixed SV-T2/OX40L or with PFA-fixed SV-T2/control cells in presence of either anti-hOX40L blocking mAb or isotype control mAb. As shown in Fig. 6, OX40 stimulation increased the levels of annexin V binding, especially in the Th1-like CD4$^+$ T cells. Since anti-OX40L mAb inhibited annexin V staining, these results suggest that under Th1-like conditions some fractions of primary CD4$^+$ T cells undergo apoptosis following OX40 stimulation.

## DISCUSSION

We show here, for the first time, that combined OX40L and TNF stimulation leads OX40$^+$ T cell lines and primary CD4$^+$ T cells to undergo apoptosis. Apoptosis-inducing effects have been described for a number of HIV-1 proteins, including Env,[46] Tat,[47] Nef,[48] Vpr,[49] and Vpu.[50] Recently, Lenardo *et al.* have shown that HIV-1 can induce necrosis of CD4$^+$ T cells.[51] However, the data presented herein, using the OX40 transfectants of the HIV-1-negative T cell line Molt-4/CCR5, clearly demonstrate that OX40-mediated cell death is independent of apoptosis- or of necrosis-inducing effects of HIV-1 proteins.

Stimulation of other DD-lacking members of the TNF-R superfamily, including TNF-R2, CD27, CD30, and CD40, induces the death of tumor cells and of normal cells under certain conditions. One known mechanism for TNF-R2-, CD30-, and CD40-induced cell death is that receptor stimulation activates cells to produce endogenous membrane TNF, which stimulates the DD-containing TNF-R1 to induce cell death.[31] A second mechanism suggested for CD40-mediated cell death is an amplification of the Fas-dependent apoptosis pathway.[52] In this study, we show that apoptosis in M/R5-OX40 cells, induced by OX40 stimulation, was efficiently blocked by the caspase inhibitor z-VAD-fmk, and was also blocked by anti-TNF-$\alpha$ neutralizing mAb. Moreover, the apoptosis of OX40-stimulated M/R5-OX40 cells was associated with the induction of endogenous TNF-$\alpha$. These results suggest that the OX40-mediated apoptosis in M/R5-OX40 cells occurs indirectly, via a TNF/TNF-R system reminiscent of that mediated via TNF-R2, CD30, and CD40.

The response to coactivation by OX40L plus TNF-$\alpha$ in Jurkat/OX40 cells is also of great interest. In Jurkat/OX40 cells, apoptosis was not induced by soluble TNF-$\alpha$ or by OX40 stimulation and endogenous TNF-$\alpha$ was not induced by OX40 stimulation, unlike the results observed in M/R5-OX40 cells. However, rapid apoptosis was induced in Jurkat/OX40 cells by costimulation with OX40L plus TNF-$\alpha$. These results suggest a new aspect of OX40 function in the induction of apoptosis in this cell line upon costimulation with OX40L plus TNF-$\alpha$. The degree to which this mechanism contributes to OX40-induced apoptosis in other cell lines, such as M/R5-OX40, CEM/OX40, U937/OX40, and THP-1/OX40, is not currently known. On the other hand, U937/OX40 and THP-1/OX40 cells were relatively resistant, and BJAB/OX40 cells were completely resistant to the combined stimulation with OX40L and TNF-$\alpha$ (Fig. 3A). Since endogenous TNF-$\alpha$ is expressed in these cells irrespec-

tive of stimulation, these cells might have an endogenous mechanism to resist TNF-$\alpha$-induced apoptosis. Furthermore, since normal B cells and monocytic cells do not express OX40, it might be possible that they lack the machinery for OX40-mediated intracellular signaling, or are equipped with an, as yet, undetermined anti-OX40 signal. Further studies are required to define the mechanisms of such resistance. In addition, since apoptosis of CEM/OX40 cells following OX40L stimulation could not be completely inhibited by the caspase inhibitor z-VAD-fmk at concentrations up to 100 $\mu$M (data not shown), it is possible that OX40-induced cell death may include additional apoptotic pathways, which may depend upon the cell line being studied.

It can be speculated that the survival or the apoptotic fate of $CD4^+$ T cells, after OX40 stimulation, is dependent on immunological environments. Kawamata *et al.* have shown that the cytoplasmic tail of OX40 binds TRAF2 and TRAF5, leading to NF-$\kappa$B activation.[12] TRAF2 is required for the TNF-mediated activation of c-Jun N-terminal kinase (JNK) and of NF-$\kappa$B, which leads to the generation of antiapoptotic signals.[3] It has been shown that TRAF2 can trigger cell death in the presence of the receptor-interacting protein (RIP), whereas in the absence of RIP, TRAF2 activates NF-$\kappa$B.[53] RIP has also been implicated in caspase-8-independent necrosis.[54] Furthermore, Li *et al.* have shown that activation of TNF-R2 induces ubiquitination and proteasomal degradation of TRAF2, leading to the enhancement of TNF-induced apoptosis.[55] In addition, it has been demonstrated that stimulation of TNF-R2, CD30, or CD40 leads to selective enhancement of TNF-R1-mediated caspase-8-dependent cell death by depletion of both TRAF2 and the antiapoptotic IAP proteins.[37] Another suggested mechanism for CD40L-mediated $CD4^+$ T cell death is failure of the induction of the antiapoptotic proteins Bcl-2 and Bcl-$X_L$.[56] However, this mechanism cannot explain OX40-mediated apoptosis, since OX40 activation has been shown to induce these two antiapoptotic proteins.[57] Recently, Ma *et al.* have shown that in both OX40 and 4-1BB-expressing cells, combined stimulation by OX40 and 4-1BB induces reduced NF-$\kappa$B activation, cell survival, and cell growth.[58] At present, it remains unclear whether OX40 activation directly mediates cell death. Taken together, it is interesting to speculate that OX40 stimulation induces cell death via an apoptotic pathway mediated by its cytoplasmic tail. Further studies are in progress to reveal the precise molecular mechanisms of OX40-induced apoptosis of T cells in various immunological environments.

In conclusion, the present study revealed a novel immunological function of OX40 in OX40-expressing $CD4^+$ T cells, with the control of cell death, in the presence of TNF, potentially resulting in a reduction of HIV-1 production.

## ACKNOWLEDGMENTS

This work was supported by grants from the Ministry of Education, Culture, Sports, Science and Technology of Japan, and the Ministry of Health, Labor and Welfare of Japan. We are grateful to Dr. A.A. Ansari (Emory University) for critical reading of this manuscript, Dr. H. Niwa (RIKEN) for the gift of the pCAGIPuro vector, and Dr. M. Baba (Kagoshima University) for the gift of the Molt-4/CCR5 cell line.

## REFERENCES

1. Latza U, Durkop H, Schnittger S, *et al.*: The human OX40 homolog: cDNA structure, expression and chromosomal assignment of the ACT35 antigen. Eur J Immunol 1994;24:677–683.
2. Mallett S, Fossum S, and Barclay AN: Characterization of the MRC OX40 antigen of activated CD4 positive T lymphocytes: A molecule related to nerve growth factor receptor. EMBO J 1990;9:1063–1068.
3. Baker SJ and Reddy EP: Modulation of life and death by the TNF receptor superfamily. Oncogene 1998;17:3261–3270.
4. Tanaka Y, Inoi T, Tozawa H, Yamamoto N, and Hinuma Y: A glycoprotein antigen detected with new monoclonal antibodies on the surface of human lymphocytes infected with human T-cell leukemia virus type-I (HTLV-I). Int J Cancer 1985;36:549–555.
5. Miura S, Ohtani K, Numata N, *et al.*: Molecular cloning and characterization of a novel glycoprotein, gp34, that is specifically induced by the human T-cell leukemia virus type I transactivator p40tax. Mol Cell Biol 1991;11:1313–1325.
6. Baum PR, Gayle RB 3rd, Ramsdell F, *et al.*: Molecular characterization of murine and human OX40/OX40 ligand systems: Identification of a human OX40 ligand as the HTLV-1-regulated protein gp34. EMBO J 1994;13:3992–4001.
7. Ohshima Y, Tanaka Y, Tozawa H, Takahashi Y, Maliszewski C, and Delespesse G: Expression and function of OX40 ligand on human dendritic cells. J Immunol 1997;159:3838–3848.
8. Stuber E, Neurath M, Calderhead D, Fell HP, and Strober W: Cross-linking of OX40 ligand, a member of the TNF/NGF cytokine family, induces proliferation and differentiation in murine splenic B cells. Immunity 1995;2:507–521.
9. Morimoto S, Kanno Y, Tanaka Y, *et al.*: CD134L engagement enhances human B cell Ig production: CD154/CD40, CD70/CD27, and CD134/CD134L interactions coordinately regulate T cell-dependent B cell responses. J Immunol 2000;164:4097–4104.
10. Imura A, Hori T, Imada K, *et al.*: The human OX40/gp34 system directly mediates adhesion of activated T cells to vascular endothelial cells. J Exp Med 1996;183:2185–2195.
11. Baba E, Takahashi Y, Lichtenfeld J, *et al.*: Functional CD4 T cells after intercellular molecular transfer of OX40 ligand. J Immunol 2001;167:875–883.
12. Kawamata S, Hori T, Imura A. Takaori-Kondo A, and Uchiyama T: Activation of OX40 signal transduction pathways leads to tumor necrosis factor receptor-associated factor (TRAF) 2- and TRAF5-mediated NF-kappa B activation. J Biol Chem 1998;273:5808–5814.
13. Flynn S, Toellner FM, Raykundalia C, Goodall M, and Lane P: CD4 T cell cytokine differentiation: The B cell activation molecule, OX40 ligand, instructs CD4 T cells to express interleukin 4 and upregulates expression of the chemokine receptor, Blr-1. J Exp Med 1998;188:297–304.
14. Ohshima Y, Yang LP, Uchiyama T, *et al.*: OX40 costimulation enhances interleukin-4 (IL-4) expression at priming and promotes the differentiation of naive human CD4(+) T cells into high IL-4-producing effectors. Blood 1998;92:3338–3345.
15. Akiba H, Miyahira Y, Atsuta M, *et al.*: Critical contribution of OX40 ligand to T helper cell type 2 differentiation in experimental leishmaniasis. J Exp Med 2000;191:375–380.
16. Tanaka H, Demeure CE, Rubio M, Delespesse G, and Sarfati M: Human monocyte-derived dendritic cells induce naive T cell differentiation into T helper cell type 2 (Th2) or Th1/Th2 effectors. Role of stimulator/responder ratio. J Exp Med 2000;192:405–412.
17. Gramaglia I, Jember A, Pippig SD, Weinberg AD, Killeen N, and Croft M: The OX40 costimulatory receptor determines the development of CD4 memory by regulating primary clonal expansion. J Immunol 2000;165:3043–3050.

18. De Smedt T, Smith J, Baum P, Fanslow W, Butz E, and Maliszewski C: OX40 costimulation enhances the development of T cell responses induced by dendritic cells in vivo. J Immunol 2002;168:661–670.
19. Bansal-Pakala P, Jember AJ, and Croft M: Signaling through OX40 (CD134) breaks peripheral T-cell tolerance. Nat Med 2001;7:907–912.
20. Valzasina B, Guiducci C, Dislich H, Killeen N, Weinberg AD, and Colombo MP: Triggering of OX40 (CD134) on CD4(+)CD25+ T cells blocks their inhibitory activity: A novel regulatory role for OX40 and its comparison with GITR. Blood 2005;105:2845–2851.
21. Imura A, Hori T, Imada K, *et al.*: OX40 expressed on fresh leukemic cells from adult T-cell leukemia patients mediates cell adhesion to vascular endothelial cells: Implication for the possible involvement of OX40 in leukemic cell infiltration. Blood 1997;89: 2951–2958.
22. Brocker T, Gulbranson-Judge A, Flynn S, Riedinger M, Raykundalia C, and Lane P: CD4 T cell traffic control: In vivo evidence that ligation of OX40 on CD4 T cells by OX40-ligand expressed on dendritic cells leads to the accumulation of CD4 T cells in B follicles. Eur J Immunol 1999;29:1610–1616.
23. Aten J, Roos A, Claessen N, Schilder-Tol EJM, Ten Berge IJM, and Weening JJ: Strong and selective glomerular localization of CD134 ligand and TNF receptor-1 in proliferative lupus nephritis. J Am Soc Nephrol 2000;11:1426–1438.
24. Ndhlovu LC, Ishii N, Murata K, Sato T, and Sugamura K: Involvement of OX40 ligand signals in the T cell priming events during experimental autoimmune encephalomyelitis. J Immunol 2001; 167:2991–2999.
25. Murata K, Nose M, Ndhlovu LC, Sato T, Sugamura K, and Ishii N: Constitutive OX40/OX40 ligand interaction induces autoimmune-like diseases. J Immunol 2002;169:4628–4636.
26. Jember AG-H, Zuberi R, Liu FT, and Croft M: Development of allergic inflammation in a murine model of asthma is dependent on the costimulatory receptor OX40. J Exp Med 2001;193:387–392.
27. Arestides RS, He H, Westlake RM, *et al.*: Costimulatory molecule OX40L is critical for both Th1 and Th2 responses in allergic inflammation. Eur J Immunol 2002;32:2874–2880.
28. Uchiyama T: Human T cell leukemia virus type I (HTLV-I) and human diseases. Annu Rev Immunol 1997;15:15–37.
29. Kopf M, Ruedl C, Schmitz N, *et al.*: OX40-deficient mice are defective in Th cell proliferation but are competent in generating B cell and CTL responses after virus infection. Immunity 1999;11: 699–708.
30. Ekkens MJ, Liu Z, Liu Q, *et al.*: The role of OX40 ligand interactions in the development of the Th2 response to the gastrointestinal nematode parasite Heligmosomoides polygyrus. J Immunol 2003;170:384–393.
31. Grell M, Zimmermann G, Gottfried E, *et al.*: Induction of cell death by tumour necrosis factor (TNF) receptor 2, CD40 and CD30: A role for TNF-R1 activation by endogenous membrane-anchored TNF. EMBO J 1999;18:3034–3043.
32. Prasad KV, Ao Z, Yoon Y, *et al.*: CD27, a member of the tumor necrosis factor receptor family, induces apoptosis and binds to Siva, a proapoptotic protein. Proc Natl Acad Sci USA 1997;94:6346–6351.
33. Mir SS, Richter BW, and Duckett CS: Differential effects of CD30 activation in anaplastic large cell lymphoma and Hodgkin disease cells. Blood 2000;96:4307–4312.
34. Lee SY, Park CG, and Choi Y: T cell receptor-dependent cell death of T cell hybridomas mediated by the CD30 cytoplasmic domain in association with tumor necrosis factor receptor-associated factors. J Exp Med 1996;183:669–674.
35. Hess S and Engelmann H: A novel function of CD40: Induction of cell death in transformed cells. J Exp Med 1996;183:159–167.
36. Chan FK and Lenardo MJ: A crucial role for p80 TNF-R2 in amplifying p60 TNF-R1 apoptosis signals in T lymphocytes. Eur J Immunol 2000;30:652–660.
37. Fotin-Mleczek M, Henkler F, Samel D, *et al.*: Apoptotic crosstalk of TNF receptors: TNF-R2-induces depletion of TRAF2 and IAP proteins and accelerates TNF-R1-dependent activation of caspase-8. J Cell Sci 2002;115:2757–2770.
38. Takahashi Y, Tanaka Y, Yamashita A, Koyanagi Y, Nakamura M, and Yamamoto N: OX40 stimulation by gp34/OX40 ligand enhances productive human immunodeficiency virus type 1 infection. J Virol 2001;75:6748–6757.
39. Biswas P, Smith CA, Goletti D, Hardy EC, Jackson RW, and Fauci AS: Cross-linking of CD30 induces HIV expression in chronically infected T cells. Immunity 1995;2:587–596.
40. Tozawa H, Andoh S, Takayama Y, *et al.*: Species-dependent antigenicity of the 34-kDa glycoprotein found on the membrane of various primate lymphocytes transformed by human T-cell leukemia virus type-I (HTLV-I) and simian T-cell leukemia virus (STLV-I). Int J Cancer 1988;41:231–238.
41. Tanaka Y, Yoshida A, Tozawa H, Shida H, Nyunoya H, and Shimotohno K: Production of a recombinant human T-cell leukemia virus type-I trans-activator (tax1) antigen and its utilization for generation of monoclonal antibodies against various epitopes on the tax1 antigen. Int J Cancer 1991;48:623–630.
42. Baba M, Miyake H, Okamoto M, Iizawa Y, and Okonogi K: Establishment of a CCR5-expressing T-lymphoblastoid cell line highly susceptible to R5 HIV type 1. AIDS Res Hum Retroviruses 2000;16:935–941.
43. Adachi A, Gendelman HE, Koenig S, *et al.*: Production of acquired immunodeficiency syndrome-associated retrovirus in human and nonhuman cells transfected with an infectious molecular clone. J Virol 1986;59:284–291.
44. Tanaka R, Yoshida A, Murakami T, *et al.*: Unique monoclonal antibody recognizing the third extracellular loop of CXCR4 induces lymphocyte agglutination and enhances human immunodeficiency virus type 1-mediated syncytium formation and productive infection. J Virol 2001;75:11534–11543.
45. Kondo K, Okuma K, Tanaka R, *et al.*: Requirements for the functional expression of OX40 ligand on human activated $CD4^+$ and $CD8^+$ T cells. Hum Immunol 2007;68:563–571.
46. Ohagen A, Ghosh S, He J, *et al.*: Apoptosis induced by infection of primary brain cultures with diverse human immunodeficiency virus type 1 isolates: Evidence for a role of the envelope. J Virol 1999;73:897–906.
47. Bartz SR and Emerman M: Human immunodeficiency virus type 1 Tat induces apoptosis and increases sensitivity to apoptotic signals by up-regulating FLICE/caspase-8. J Virol 1999;73:1956–1963.
48. Xu X-N, Laffert B, Screaton GR, *et al.*: Induction of Fas ligand expression by HIV involves the interaction of Nef with the T cell receptor zeta chain. J Exp Med 1999;189:1489–1496.
49. Hrimech M, Yao XJ, Bachand F, Rougeau N, and Cohen EA: Human immunodeficiency virus type 1 (HIV-1) Vpr functions as an immediate-early protein during HIV-1 infection. J Virol 1999;73: 4101–4109.
50. Casella CR, Rapaport EL, and Finkel TH: Vpu increases susceptibility of human immunodeficiency virus type 1-infected cells to fas killing. J Virol 1999;73:92–100.
51. Lenardo MJ, Angleman SB, Bounkeua V, *et al.*: Cytopathic killing of peripheral blood CD4 (+) T lymphocytes by human immunodeficiency virus type 1 appears necrotic rather than apoptotic and does not require env. J Virol 2002;76:5082–5093.
52. Afford SC, Ahmed-Choudhury J, Randhawa S, *et al.*: CD40 activation-induced, Fas-dependent apoptosis and NF-kappaB/AP-1 signaling in human intrahepatic biliary epithelial cells. FASEB J 2001;15:2345–2354.

53. Pimentel-Muinos FX and Seed B: Regulated commitment of TNF receptor signaling: A molecular switch for death or activation. Immunity 1999;11:783–793.
54. Holler N, Zaru R, Micheau O, *et al.*: Fas triggers an alternative, caspase-8-independent cell death pathway using the kinase RIP as effector molecule. Nat Immunol 2000;1:489–495.
55. Li X, Yang Y, and Ashwell JD: TNF-RII and c-IAP1 mediate ubiquitination and degradation of TRAF2. Nature 2002;416:345–347.
56. Blair PJ, Riley JL, Harlan DM, *et al.*: CD40 ligand (CD154) triggers a short-term CD4(+) T cell activation response that results in secretion of immunomodulatory cytokines and apoptosis. J Exp Med 2000;191:651–660.
57. Rogers PR, Son J, Gramaglia I, Killeen N, and Croft M: OX40 promotes Bcl-xL and Bcl-2 expression and is essential for long-term survival of CD4 T cells. Immunity 2001;15:445–455.
58. Ma BY, Mikolajczak SA, Danesh A, *et al.*: The expression and the regulatory role of OX40 and 4-1BB heterodimer in activated human T cells. Blood 2005;106:2002–2010.

Address reprint requests to:
*Yuetsu Tanaka*
*Department of Immunology*
*Graduate School of Medicine*
*University of the Ryukyus*
*Uehara 207*
*Nishihara, Okinawa 903-0215, Japan*

*E-mail:* yuetsu@s4.dion.ne.jp

MAJOR ARTICLE

# Interleukin-4–Transgenic hu-PBL-SCID Mice: A Model for the Screening of Antiviral Drugs and Immunotherapeutic Agents against X4 HIV-1 Viruses

**Kazu Okuma,[1] Reiko Tanaka,[1] Tomoyuki Ogura,[2] Mamoru Ito,[2] Sei Kumakura,[3] Mikiro Yanaka,[3] Masako Nishizawa,[4] Wataru Sugiura,[4] Naoki Yamamoto,[4] and Yuetsu Tanaka[1]**

[1]Department of Immunology, Graduate School and Faculty of Medicine, University of the Ryukyus, Okinawa, [2]Central Institute for Experimental Animals, Kanagawa, and [3]Kureha Corporation and [4]National Institute of Infectious Diseases, Tokyo, Japan

**CXCR4-tropic (X4) human immunodeficiency virus type 1 (HIV-1) does not efficiently infect and replicate in severe combined immunodeficiency (SCID) mice reconstituted with human peripheral blood mononuclear cells, termed "hu-PBL-SCID mice," due to, at least in part, relatively low levels of expression of the CXCR4 coreceptor. To overcome this limitation, interleukin (IL)–4–transgenic hu-PBL-SCID mice were derived that spontaneously synthesized human IL-4, which has been shown to enhance CXCR4 expression and promote X4 virus infection in vitro. Experiments reported here show that (1) synthesis of human IL-4 in vivo augmented CXCR4 expression on human CD4$^+$ lymphocytes and importantly led to productive infection of not only X4 HIV-$1_{NL4-3}$ but also multidrug-resistant primary clinical isolates and that (2) the in vivo infection could be significantly blocked by the administration of a CXCR4 antagonist. Altogether, IL-4–transgenic hu-PBL-SCID mice provide a useful model for X4 HIV-1 study and testing/screening of anti-X4 viral drugs.**

HIV-1 isolates enter target cells primarily after binding to the CD4 receptor and via the CXCR4 and CCR5 coreceptors [1–5] and are classified into X4 and R5 strains, respectively [6]. The X4 isolates are frequently implicated in the decline of peripheral CD4$^+$ T cell counts characteristic of the late stage of HIV-1 infection proceeding to the development of AIDS [7].

hu-PBL-SCID mice have been extensively used as a small animal model to study HIV-1 pathogenesis [8–14]. Results from a previous study showed that, although infection of human peripheral blood mononuclear cell (PBMC)–reconstituted hu-PBL-SCID mice with a predominantly R5 HIV-1 caused intensive CD4$^+$ T cell depletion, infection of similarly reconstituted mice with the same infectious dose of an X4 HIV-1 resulted in little or no CD4$^+$ T cell depletion [11]. Thereafter, it was noted that this limitation of X4 HIV-1 infection was due, at least in part, to a decrease in the intensity of CXCR4 expression on CD4$^+$ T cells [13]. Thus, it was reasoned that the pathogenic effects of the X4 HIV-1 strains in the hu-PBL-SCID mice might be related to the relative levels of the expression of HIV-1 coreceptor (the state of activation/differentiation) on human CD4$^+$ T cells at the time of infection in these mice. This limitation has to date restricted our ability to use this mouse model for understanding the mechanisms of X4 HIV-1 pathogenesis and for the evaluation of candidate therapeutics against X4 viruses. These findings prompted us to seek alternative strategies for the development of an improved hu-PBL-SCID mouse system that is permissive for infection/replication of X4 isolates.

Human interleukin (IL)–4 has been shown to specifically enhance the cell-surface expression of CXCR4 on

Received 1 May 2007; accepted 11 July 2007; electronically published 4 December 2007.

Potential conflicts of interest: none reported.

Presented in part: First International Workshop on Humanized Mice, Tokyo, 11–12 October 2006 (abstract P-15); 14th Conference on Retroviruses and Opportunistic Infections, Los Angeles, 25–28 February 2007 (abstract 496).

Financial support: Health and Labor Science Research Grant (Research on Publicly Essential Drugs and Medical Devices) from the Ministry of Health, Labor, and Welfare of Japan (grant H16-soyaku-004).

Reprints or correspondence: Dr. Kazu Okuma, Dept. of Immunology, Graduate School and Faculty of Medicine, University of the Ryukyus, Uehara 207, Nishihara-cho, Nakagami-gun, Okinawa 903-0215, Japan (kokuma@med.u-ryukyu.ac.jp).

**The Journal of Infectious Diseases 2008; 197:134–41**

0022-1899/2008/19701-0021$15.00
DOI: 10.1086/524303

resting peripheral blood T cells [15]. Furthermore, it has been reported that human IL-4 plays an important role in rendering $CD4^+$ T cells susceptible to X4 HIV-1 infection via enhanced cell-surface expression of the CXCR4 coreceptor in vitro [15–17].

In efforts to overcome the limitation inherent with the use of hu-PBL-SCID mice for the study of X4 HIV-1 as described above, we developed an IL-4–transgenic immunodeficient mouse model that consistently secreted readily detectable serum levels of human IL-4. We show here that X4 isolates readily infect/replicate in this mouse model but not in wild-type (wt) non–IL-4–transgenic mice and that this model can now be exploited for the rapid evaluation of the therapeutic efficacy of new anti-X4 HIV-1 agents in vivo.

## METHODS

***IL-4–producing mice.*** Two strains of human IL-4–transgenic immunodeficient mice were bred on the C.B-17-*scid* [18] and BALB/cA-Rag2$^{-/-}\gamma_c^{-/-}$ (dKO) genetic background mice [19, 20] at the Central Institute for Experimental Animals (CIEA) as follows. PBMCs were isolated from a healthy human volunteer and activated in vitro with pokeweed mitogen. RNA was prepared from these PBMCs, and then cDNA was synthesized by reverse-transcriptase polymerase chain reaction (PCR). Human IL-4 cDNA was amplified from the cDNA using one set of primers: 5'-CCCGGGATCGTTAGCTTCTCCTGATAAAA-3' and 5'-GCGGCCGCTATTCAGCTCGAACACTTTGAAT-3'. The product was inserted into the PCR2.1 vector by use of the TA cloning kit (Invitrogen) and the insert sequenced. After confirmation of the sequence, IL-4 cDNA was inserted into pCMVb with a CMV promoter (Invitrogen). To produce transgenic mice, a DNA fragment containing the CMV promoter, IL-4 cDNA, and Poly(A) regions was excised with *Xho*I and *Hind*III sites of pCMVb and microinjected into the pronuclei of fertilized eggs from the 2 strains (C.B-17-*scid* and BALB/cA-dKO) of mice. These eggs were subsequently transplanted into oviducts of pseudopregnant foster recipient mice. The offspring mice were screened to confirm the insertion of the transgene into the genome by PCR, and serum from these mice was screened for levels of human IL-4 by ELISA with a commercial kit (BD). The IL-4 transgene–hemizygous mice were maintained by mating them with wt mice with the same genetic background in the specific-pathogen–free (SPF) facility of the CIEA. The mice were transferred to the SPF and biosafety level 3 facilities of the Institute for Animal Experiments, University of the Ryukyus, and were used for further experiments. The experimental protocols were approved by the Institutional Animal Care and Use Committee on the basis of the Regulation for Animal Experimentation of the CIEA and University of the Ryukyus before the initiation of the study.

***Viruses.*** X4 HIV-$1_{NL4-3}$ was obtained as described elsewhere [14]. Fourteen multidrug-resistant (MDR) HIV-1 clinical isolates were obtained from HIV-1–infected patients who had been treated with highly active antiretroviral therapy (HAART). The viruses were propagated in PBMCs stimulated with phytohemagglutinin (PHA; Sigma), IL-2 (National Institutes of Health AIDS Research and Reference Reagent Program), and IL-4 (Peprotec). Three isolates from these MDR isolates that efficiently grew in the activated cells were selected for further experiments. The titers of virus stocks were determined by end-point titration using a 2-fold limiting dilution of the stock and in vitro PHA-activated human PBMCs, and the infectious units (IU) were calculated.

***CXCR4 antagonist.*** The synthesis and purification of the CXCR4 antagonist KRH-1636 were performed at Kureha Corporation as described elsewhere [21]. As a control, the carrier tartrate was used in parallel.

***Transplantation and infection.*** The control (wt) and the IL-4–transgenic C.B-17-*scid* mice were depleted of NK cells by the intraperitoneal (ip) injection of 0.5–1.0 mg of anti–mouse IL-2R $\beta$ (TM$\beta$-1) [22] per animal. The IL-4–transgenic and the control BALB/cA-dKO mice do not require TM$\beta$-1 treatment because they lack NK cells [19, 20]. PBMCs were isolated from healthy human donors. Groups of 2–4-month-old IL-4–transgenic mice from each of the 2 background strains and their corresponding non–IL-4–transgenic wt mice were injected ip with PBMCs 3 days later. Groups of mice were challenged 24 h later ip with mock, HIV-$1_{NL4-3}$, or MDR isolates (2000 IU/500 $\mu$L/animal). For the experiments using the CXCR4 antagonist, groups of mice were administered 0.1 mL of 10 mmol/L KRH-1636, the tartrate carrier or saline ip at 1 h before and 1 day after virus infection. At 6–8 days after infection, the mice were killed, their blood was obtained by cardiocentesis, and human lymphocytes were collected from the peritoneal lavage fluids. The serum samples were assayed for levels of human IL-4 by use of an ELISA kit (R&D Systems). The human lymphocytes were analyzed using flow cytometry as described below. The remaining cells were cultured in RPMI 1640 medium (Sigma) supplemented with fetal calf serum and IL-2. The peritoneal lavage fluids, serum samples, and lymphocyte culture supernatants were examined for levels of p24 by use of an ELISA kit (Zepto Metrix).

***Flow cytometry analysis.*** Cell samples to be analyzed by flow cytometry were initially incubated with normal human IgG for blocking of the Fc receptors. For cell-surface staining, aliquots of cells were then stained with Cy5-labeled anti-CD4 (OKT4) and phycoerythrin-labeled anti-CXCR4 (12G5; Dako) or with Cy5-labeled anti-CD3 (OKT3). For intracellular staining, after CD3 staining the aliquots of cells were fixed, permeabilized, and incubated with fluorescein isothiocyanate–labeled anti–HIV-1 Gag p24 (2C2; Y.T. et al., unpublished data). Stained samples were analyzed on a FACSCalibur flow cytometer, using Cell Quest software (BD Pharmingen). Aliquots of cells stained

**Table 1. Expression of human CD4, CXCR4, and intracellular HIV-1 p24 in cells from X4 HIV-1–infected hu-PBL-SCID mice.**

| Category | X4 HIV-1 infection | Mice, no. | $CD4^+$ T cells, % | *P* | $CXCR4^+CD4^+$ T cells, % | *P* | $p24^+$ T cells, % | *P* |
|---|---|---|---|---|---|---|---|---|
| C.B-17-*scid* mice | | | | | | | | |
| Control | NL4-3 | 6 | 22.1 ± 8.3 | <.001 | 45.2 ± 4.7 | <.001 | 0.1 ± 0.1 | NS |
| IL-4 transgenic | NL4-3 | 6 | 66.3 ± 9.0 | | 65.5 ± 6.1 | | 0.1 ± 0.1 | |
| BALB/cA-dKO mice | | | | | | | | |
| Control | NL4-3 | 5 | 35.9 ± 5.1 | <.01 | 32.6 ± 1.4 | <.001 | 0.2 ± 0.1 | <.05 |
| IL-4 transgenic | NL4-3 | 3 | 57.4 ± 8.3 | | 68.2 ± 3.9 | | 3.2 ± 1.2 | |

**NOTE.** Cells in peritoneal lavage fluid from control and interleukin (IL)–4–transgenic hu-PBL-SCID mice on either the C.B-17-*scid* or BALB/cA-dKO background were labeled with appropriate monoclonal antibodies and analyzed by flow cytometry, as described in Methods. Analyzed data are shown as mean ± SD values. NS, not significant. The indicated *P* values for the comparison of control vs. transgenic mice for each category are based on Student's *t* test.

with or without each of the antibodies described above were used as controls for the purposes of establishing gates and for the determination of the frequency of positive cells.

***Statistical analysis.*** Data obtained by flow cytometry were analyzed by Student's *t* test with GraphPad Prism (version 4.0c for Mac OS X; GraphPad Software).

## RESULTS

***Production of human IL-4 in IL-4–transgenic mice.*** Efforts to construct the IL-4–transgenic mice constitutively synthesizing human IL-4 finally led to the establishment of mice on each of the 2 immunodeficient backgrounds expressing either high or low serum levels of human IL-4 (data not shown). On the basis of preliminary data obtained on the efficiency of virus replication, all subsequent experiments were done using only the 2 strains with high serum IL-4 expression levels. We assayed for levels of human IL-4 in the serum from the $IL\text{-}4^+$ hu-PBL-SCID mice and the wt hu-PBL-SCID mice on either the C.B-17-*scid* or BALB/cA-dKO background after infection with X4 $HIV\text{-}1_{NL4\text{-}3}$. Serum from each of the IL-4–transgenic mice on either background contained significant levels of human IL-4 (~800–1800 pg/mL), whereas serum from the control mice on the same background showed nondetectable levels of human IL-4. These data demonstrate that the human IL-4 synthesized by the IL-4–transgenic mice is generated from the transgene but not from the human PBMCs transplanted in these mice.

***Effect of human IL-4 on the levels of human CXCR4 and CD4 expression by cells transplanted into mice.*** Since human IL-4 has been previously documented to enhance the expression of CXCR4 in vitro, experiments were done to examine the expression of human CXCR4 on transplanted $CD4^+$ cells in the peritoneal lavage fluids from $HIV\text{-}1_{NL4\text{-}3}$–infected $IL\text{-}4^+$ hu-PBL-SCID mice and control hu-PBL-SCID mice on either the C.B-17-*scid* or BALB/cA-dKO background. There did not appear to be any detectable difference in the absolute amounts of cells recovered from the peritoneal lavage fluids from the IL-4–positive or IL-4–negative hu-PBL-SCID mice on either background (data not shown). Flow cytometry analysis demonstrated that the frequency of human $CD4^+$ cells from the IL-4–transgenic C.B-17-*scid* or BALB/cA-dKO mice was significantly higher than that from the control mice (table 1). As expected, there was a marked increase in the frequency of CXCR4-expressing $CD4^+$ cells from the IL-4–transgenic mice on either genetic background relative to that from the control mice (figure 1*A* and table 1). Thus, these data indicate that human IL-4 produced endogenously is functional in vivo in terms of its ability to enhance human CXCR4 expression on $CD4^+$ cells transplanted into the mice.

***Increased frequency of X4 HIV-1–infected cells from IL-4–transgenic hu-PBL-SCID mice.*** Since the constitutive synthesis of human IL-4 in IL-4–transgenic hu-PBL-SCID mice resulted in the enhanced expression of X4 HIV-1 receptors (human CXCR4/CD4) on the transplanted cells, we reasoned that such cells were likely to be more permissive to the infection and replication of X4 HIV-1. We thus challenged the IL-4–transgenic hu-PBL-SCID mice and control hu-PBL-SCID mice bred on the C.B-17-*scid* or BALB/cA-dKO mice with $HIV\text{-}1_{NL4\text{-}3}$. Cells obtained from the peritoneal lavage fluids were analyzed for cell-surface expression of human CD3 (since HIV-1 downmodulates CD4 expression) and the presence of intracellular p24. As seen in figure 1*B* and table 1, although very few if any $CD3^+$ cells from the control or IL-4–transgenic C.B-17-*scid* mice showed p24 expression, there was a >10-fold increase in the frequency of $CD3^+$ T cells that expressed p24 from the IL-4–transgenic BALB/cA-dKO mice relative to the control mice. These data suggest that, while transgene-induced human IL-4 increases the frequency of $CD4^+CXCR4^+$ T cells transplanted into both the C.B-17-*scid* and the BALB/cA-dKO mice, only the latter demonstrates increased sensitivity to X4 HIV-1 infection and replication, at least when this assay is used (see below).

***High production of X4 HIV-1 in the culture supernatants of cells from IL-4–transgenic hu-PBL-SCID mice.*** In an effort

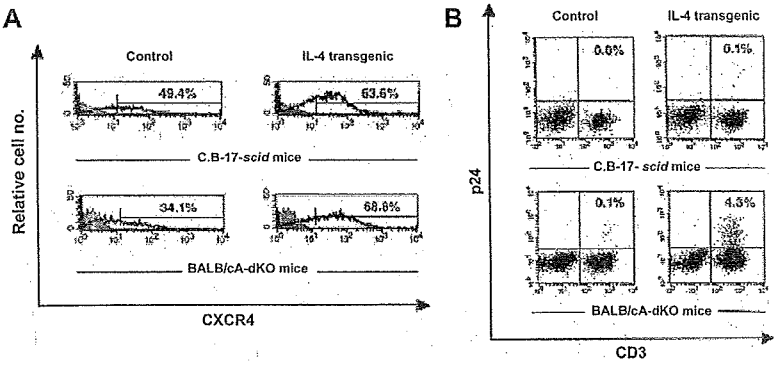


**Figure 1.** Enhancement of the expression of CXCR4 coreceptor and facilitation of X4 HIV-1 infection and replication in hu-PBL-SCID mice by in vivo production of human interleukin (IL)–4. Groups of hu-PBL-SCID mice, generated from IL-4–transgenic and nontransgenic (control) mice on either the C.B-17-*scid* or BALB/cA-dKO background, were injected intraperitoneally with HIV-$1_{NL4-3}$ at ~24 h after peripheral blood mononuclear cell (PBMC) reconstitution. Six to eight days later, peritoneal lavage fluids were harvested from mice in each group, and cells were collected from the fluids by density-gradient centrifugation. *A*, Cells analyzed for the frequency and mean density of human CXCR4 expression on $CD4^+$ cells by flow cytometry. Data for analyzed cells are depicted by a thick line, and the background control profile is depicted by a thin line and gray shading. The nos. above the bars represent the percentage of positive cells. Data shown are representative of mice in each group from 3 independent experiments. *B*, HIV-1 infectivity. Cells were subjected to flow cytometry after cell-surface CD3 and intracellular p24 staining. Analyzed data are depicted as dot plots. The nos. in the graphs indicate the percentage of $CD3^+p24^+$ cells. Data displayed are representative of mice in each group from 3 independent experiments.

to determine the reason for our failure to detect levels of intracellular p24 in the IL-4–transgenic mice on the C.B-17-*scid* background and to further support the above finding, peritoneal lavage fluids were collected from mock- or HIV-$1_{NL4-3}$–infected $IL\text{-}4^+$ hu-PBL-SCID mice and, for purposes of control, the HIV-$1_{NL4-3}$–infected non–IL-4–transgenic mice on the C.B-17-*scid* background. The cells were isolated from the peritoneal lavage fluids, and an aliquot was analyzed for the frequency and the relative density of human CXCR4/CD4; the remaining aliquot was cultured in vitro. In addition, the peritoneal lavage fluids and the culture supernatants of cells at days 1–3 after culture were assayed for levels of p24 production. As displayed in table 2, although the frequency of $CXCR4^+CD4^+$ cells in the IL-4–transgenic mice was significantly higher than that in the nontransgenic mice, the mean fluorescence intensity (MFI) of CXCR4 expressed by the $CD4^+$ T cells from these mice was not increased compared with the control (because of an increase in the frequency of $CXCR4^+CD4^+$ cells with relatively low MFI; see figure 1*A*). Analysis of levels of synthesized p24 demonstrated marked differences, as shown in figure 2. Thus, although the amounts of p24 produced were modest in the peritoneal lavage fluids and the cell-culture supernatants from HIV-1–infected control mice, the levels of p24 produced by those from HIV-1–infected IL-4–transgenic mice were strikingly higher (15,429, 11,844, 1696, and 53 pg/mL in the supernatants on day 3) (mean, 48.9 vs. 7255 pg/mL; >100-fold increase). Although the levels of p24 produced by one of the IL-4–transgenic mice (mouse 12) were similar to those in the control mice, this was likely due to the much lower relative level of human IL-4 (354 pg/mL in serum) produced by mouse 12 than those from the other 3 IL-4–transgenic mice (4227, 6313, and 2356 pg/mL in serum). The present data not only document the fact that the cells from these

**Table 2. Effect of the CXCR4 antagonist KRH-1636 on the expression of human CXCR4 by $CD4^+$ cells from X4 HIV-1–infected interleukin (IL)–4–transgenic hu-PBL-SCID mice.**

| C.B-17-*scid* mice | X4 HIV-1 Infection | CXCR4 antagonist | Mice, no. | $CXCR4^+CD4^+$ T cells, % | *P* | CXCR4 on $CD4^+$ T cells, MFI | *P* |
|---|---|---|---|---|---|---|---|
| Control | NL4-3 | Mock | 4 | 45.5 ± 9.3 | <.05[a] | 73.7 ± 36.0 | NS[a] |
| IL-4 transgenic | NL4-3 | Mock | 4 | 66.7 ± 7.4 | NS[b] | 73.1 ± 6.2 | <.05[b] |
| IL-4 transgenic | NL4-3 | KRH-1636 | 4 | 63.0 ± 4.2 | ... | 62.2 ± 4.8 | ... |

**NOTE.** Control or IL-4–transgenic hu-PBL-SCID mice on the C.B-17-*scid* background infected with X4 HIV-$1_{NL4-3}$ were administered mock KRH-1636 or real KRH-1636. Cells isolated from the peritoneal lavage fluid from the mice in each group were labeled with appropriate monoclonal antibodies and subjected to flow cytometry, as described in Methods. Data analyzed are displayed as mean ± SD values. MFI, mean fluorescence intensity; NS, not significant. The indicated *P* values are based on Student's *t* test.

[a] For the comparison between control mice and IL-4–transgenic mice that received a mock CXCR4 antagonist.

[b] For the comparison between IL-4–transgenic mice that received a mock CXCR4 antagonist and IL-4–transgenic mice that received KRH-1636.